Aus dem Lehrstuhl der Mikrobiologie

Prof. Dr. Dr. André Gessner
der Fakultät für Medizin
der Universität Regensburg

SARS-CoV-2 Evolution in Critically Ill Patients with Prolonged Infections Requiring Intubation or ECMO

Inaugural – Dissertation

zur Erlangung des Doktorgrades

der Medizin

der
Fakultät für Medizin
der Universität Regensburg

vorgelegt von
Tanja Kraft

2026

Aus dem Lehrstuhl der Mikrobiologie

Prof. Dr. Dr. André Gessner
der Fakultät für Medizin
der Universität Regensburg

SARS-CoV-2 Evolution in Critically Ill Patients with Prolonged Infections Requiring Intubation or ECMO

Inaugural – Dissertation

zur Erlangung des Doktorgrades

der Medizin

der
Fakultät für Medizin
der Universität Regensburg

vorgelegt von
Tanja Kraft

2026

Dekan:	Prof. Dr. Dirk Hellwig
1. Berichterstatter:	Prof. Dr. Barbara Schmidt
2. Berichterstatter:	PD Dr. Clemens Wiest
Tag der mündlichen Prüfung:	18.09.2026

ליחיד

(For the One)

Index

1. Abstract 9
2. Zusammenfassung 10
3. Introduction 11
3.1. Origin of SARS-CoV-2 11
3.2. Genome structure and virion composition 12
3.3. Virus host interaction and immune response 13
3.4. Symptomatology and clinical outline of COVID-19 15
3.5. Therapeutic strategies 16
3.6. Evolution of SARS-CoV-2 – VOCs 19
3.7. Aim and objectives 21
4. Material and Methods 22
4.1. Material 22
4.1.1. SARS-CoV-2 oligonucleotides 24
4.2. Methods 24
4.2.1. Molecular biology 24
4.2.2. Clinical data assembly 26
4.2.3. COVUR study 27
4.2.4. SARS-CoV-2 PEPperChip peptide microarray 28
4.2.5. Statistical analysis, graph compilation and use of translation tools 29
5. Results - Study of SARS-CoV-2 evolution *in vivo* 30
5.1. Clinical characteristics of the patient cohort at hospital admission 30
5.2. Laboratory parameters at admission of the patients 32
5.3. Clinical follow-up of the patients upon treatment 34

5.4. Disease progression based on virological parameters shows an inverse correlation between viral load and immune response 36
5.5. Virological profile reveals that most patients experienced a viremic phase 42
5.6. Genome sequencing identifies mutational hotspot in viral polymerase 43
5.7. Epitope mapping reveals varying reasons for amino acid mutations 47
5.8. Comparison between patient groups highlights treatment as highly influential on the occurrence of mutations 51
5.9. Univariate regression model identifies several significant parameters 53
5.10. Multivariate regression analysis highlights the influence of replication duration and patient age as key factors 55
6. Discussion 56
6.1. Patient cohort confirms suspected risk factors for severe COVID-19 disease progression 56
6.2. Elevated CRP and D-Dimer levels are prognostic indicators for critical COVID-19 57
6.3. IgG positivity at hospitalization detected in the majority of cases 58
6.4. Amino acid exchange hotspots detected in spike protein and viral polymerase 60
6.5. Epitope mapping emphasizes individuality of mutations according to course of disease 63
6.6. Duration of replication correlates with occurrence of mutation events 66
7. Conclusion 69
8. Appendix 71
8.1. Supplementary Figures 71
8.2. List of Figures 74
8.3. List of Tables 75
8.5. List of abbreviations 76
Preprint 77

Literaturverzeichnis 78

Eidesstattliche Erklärung 91

1. Abstract

The outbreak of SARS-CoV-2 in December 2019 and the ensuing global pandemic raised critical questions about the virus's capacity for rapid adaptation to environmental conditions. In this study, we investigated viral evolution in critically ill patients suffering from severe lung failure. From November 2020 to December 2022, respiratory samples were collected from a total of 41 patients upon admission to the intensive care unit at the University Hospital Regensburg, Germany, and during the course of treatment (median interval: 15 days; range: 6 to 42 days). The samples were analyzed for genomic alterations using next-generation sequencing. Detected changes were correlated with clinical, virological, immunological, and therapeutic parameters using both univariate and multivariate logistic regression analysis.

Seventeen of 41 patients (41%) developed amino acid substitutions in non-structural proteins (nsp) 2, 3, 4, 10, 14, and 15, as well as in open reading frames 3a and 8, and within the spike and nucleocapsid proteins over the course of the study. Notably, 20 of 27 observed changes represented reversions to the Wuhan-1 wild-type genome, including eight at position 323 of the polymerase nsp12. Statistically significant factors associated with the occurrence of mutations included younger age, prolonged stay in the intensive care unit, ECMO and catecholamine treatment, development of thrombosis, extended virus replication period, and infection with the Delta variant ($p<0.05$). In contrast, treatment with remdesivir was negatively correlated with the emergence of mutations. Epitope mapping revealed that the humoral immune response was unlikely to be the main driver of viral evolution *in vivo*.

Thus, the likelihood of genomic alterations in severely ill patients increases with both disease severity and duration of virus replication. The frequent observation of reversions to the wildtype genome suggests that the virus preferentially replicates in inflamed and poorly ventilated areas of the lungs – an effect that may be further amplified by the presence of pulmonary embolism. Furthermore, replication appears to be suppressed by the administration of remdesivir. These findings highlight that integrating antiviral strategies into the clinical management of severely ill patients may limit the emergence of potentially novel mutations.

2. Zusammenfassung

Der Ausbruch von SARS-CoV-2 im Dezember 2019 und die nachfolgende globale Pandemie warfen kritische Fragen auf, inwiefern sich das Virus rasch an Umweltbedingungen anpassen kann. In unserer Studie haben wir die SARS-CoV-2 Evolution in kritisch kranken Patienten mit schwerer Lungeninsuffizienz untersucht. Von November 2020 bis Dezember 2022 wurden von 41 Patienten respiratorische Proben bei Aufnahme in das Universitätsklinikum Regensburg, Deutschland, sowie im Verlauf der Behandlung abgenommen (Intervall im Median 15 Tage, Spannbreite 6 bis 42 Tage) und mittels *Next-Generation Sequencing* auf Aminosäure-Austausche untersucht. Die nachgewiesenen Veränderungen wurden anschließend mit klinischen, virologischen, immunologischen und therapeutischen Parametern mittels univariater und multivariater logistischer Regressionsanalyse korreliert.

Siebzehn der 41 Patienten (41%) entwickelten über die Dauer der Untersuchung Veränderungen in den Nicht-Strukturproteinen (nsp) 2, 3, 4, 10, 14, und 15, sowie den *Open reading frames* 3a und 8 und innerhalb der Spike- und Nukleokapsid-Proteine. Bemerkenswerterweise handelte es sich bei 20 der 27 Veränderungen um eine Reversion zum Wuhan-1 Wildtyp-Genom. Acht dieser Rückmutationen traten an Position 323 der Polymerase nsp12 auf. Parameter, die mit dem Auftreten von Mutationen statistisch signifikant korrelierten, waren jüngeres Alter, längerer Aufenthalt auf der Intensivstation, ECMO- und Katecholamin-Behandlung, Auftreten von Thrombosen, längere Virusreplikation und Infektion mit der Delta-Variante ($p<0.05$). Dagegen war die Behandlung mit Remdesivir mit dem Auftreten von Mutationen negativ korreliert. Ein Epitop-Mapping zeigte, dass die humorale Immunantwort vermutlich nicht der entscheidende Faktor für die virale Evolution *in vivo* war.

Aminosäure-Austausche im SARS-CoV-2 Genom treten also bei schwer kranken Patienten mit zunehmender Krankheitsschwere und Replikationsdauer des Virus gehäuft auf. Die beobachteten Rückmutationen zum Wildtyp lassen vermuten, dass sich SARS-CoV-2 in entzündeten und minderbelüfteten Lungenabschnitten bevorzugt vermehrt – ein Effekt, der durch das Vorhandensein einer Lungenembolie zusätzlich verstärkt werden könnte. Durch die Gabe von Remdesivir wird das Virus an der

Replikation gehindert. Diese Ergebnisse unterstreichen die Rolle der antiviralen Therapie bei der Vorbeugung möglicher Neumutationen in schwer erkrankten Patienten.

3. Introduction

3.1. Origin of SARS-CoV-2

As a new virus emerged in Wuhan, China, at the end of 2019, it was soon classified as a member of the Coronaviridae (Wu et al. 2020b). On February 11, 2020, the International Committee on Taxonomy of Viruses named the virus Severe Acute Respiratory Syndrome Coronavirus 2 or 'SARS-CoV-2' (Gorbalenya et al. 2020). The associated disease was called Coronavirus Disease 2019 (COVID-19) by the WHO (World Health Organization).

While the COVID-19 pandemic has undeniably shaken society and our health care systems in an unprecedented way, other coronaviruses, such as SARS (Severe Acute Respiratory Syndrome) and MERS (Middle East Respiratory Syndrome), have caused outbreaks with global spread in the last two decades (Drosten et al. 2003; Zaki et al. 2012).

SARS-CoV-2 emerged in the province Hubei, Wuhan, China and quickly spread around the globe (Wu et al. 2020b). Its origin has been subject to discussion ever since its discovery. Definitive evidence of animal-to-human cross-species spillover as the source of SARS-CoV-2 still requires further investigation. Notably, coronavirus sequences with high similarity to SARS-CoV-2 have been detected in bats, suggesting potential links to this species as an evolutionary precursor (Zhou et al. 2020). Additionally, virus isolates from pangolins have demonstrated homology in large parts of their genome. Unlike bats, which do not exhibit symptoms upon infection, pangolins show an inflammatory response and clinical signs of disease. Thus, pangolins may serve as intermediate hosts, possibly playing a role in viral adaption and genomic changes (Xiao et al. 2020).

3.2. Genome structure and virion composition

SARS-CoV-2 is an enveloped virus with a single stranded, positive sense ribonucleic acid (RNA) genome comprising 29.903 nucleotides (Kim et al. 2020) and 11 open reading frames (ORF). ORF1ab and ORF1b are located near the 5´ terminus and encode 16 non-structural proteins (nsp), which are formed through autoproteolytic cleavage. While many of these nsps have functions that are not yet fully understood, some of them have been investigated in more detail in relation to other coronaviruses. For example, nsp12 serves as the RNA-dependent RNA-polymerase (RdRP) catalyzing the elongation of RNA by incorporating nucleotides complementary to the viral RNA template. Nsp13 functions as helicase and nsp14 as exonuclease, which collectively form the RNA-synthesizing complex (Snijder et al. 2016).

The 3´ terminus is organized to encode four structural proteins, namely spike, envelope, membrane and nucleocapsid proteins, which form the virion structure, as well as eight accessory proteins, 3a, 3b, p6, 7a, 7b, 8b, 9b, and orf14 (Wu et al. 2020a). Spike, envelope and membrane proteins are located on the surface of the virion. The spike protein plays an important role in host cell entry but is also predominantly targeted by the host immune system. The nucleocapsid protein by contrast encapsidates the RNA genome, forming the ribonucleoprotein complex (Liang et al. 2020).

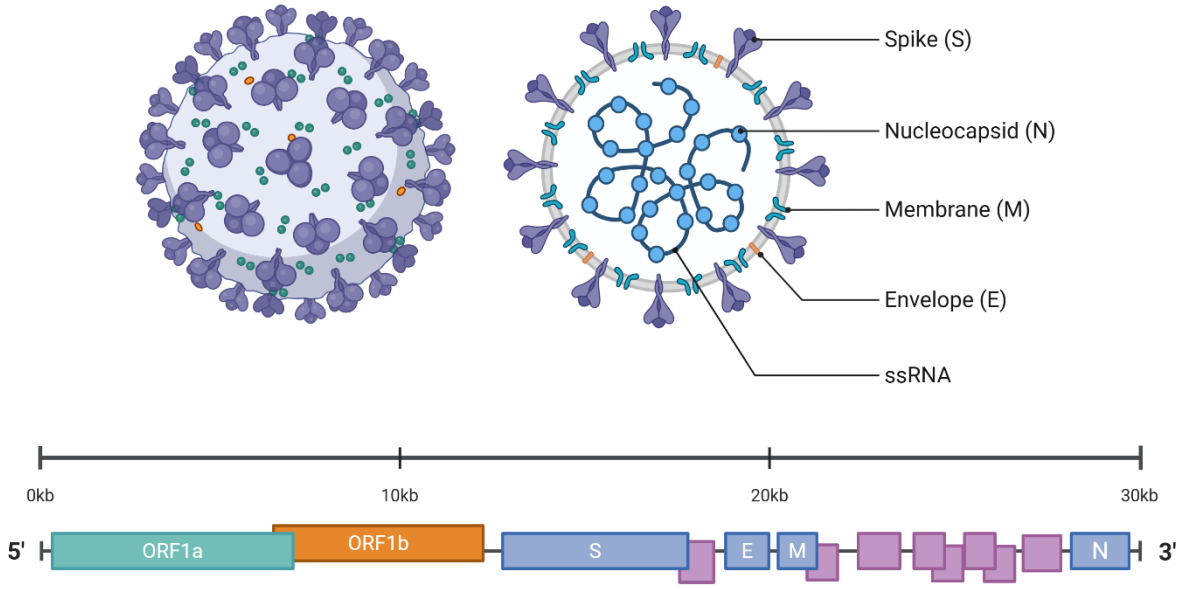


Figure 1 Genome organization of SARS-CoV-2*. The virion structure consists of structural proteins called spike (S), membrane (M), envelope (E) and nucleocapsid (N) proteins. The genome also codes for non-structural proteins (nsp), which play important roles in viral replication and transmission. ORF, open reading frame; kb, kilobase; ss, single strand; RNA, ribonucleic acid. Modified from (Kim et al. 2020), this graph was created using BioRender.com.*

3.3. Virus host interaction and immune response

Viruses depend on host organisms to replicate and spread new virions. Similar to SARS-CoV, SARS-CoV-2 utilizes the Angiotensin-converting-enzyme-2 (ACE2) as its specific receptor, located on the extracellular part of the cell membrane (Li et al. 2003). In order to invade a cell, the spike protein on the virus surface binds to ACE2, leading to the formation of a fusion complex that results in membrane coalescence (Essalmani et al. 2022), as described for other coronaviruses (Gallagher und Buchmeier 2001). Viral entry is dependent on the expression of ACE2 and the presence of host cell transmembrane proteases like TMPRSS2, allowing infection only in cells that express both. Co-expression of both molecules is found, among others, in type II pneumocytes and nasal goblet secretory cells (Ziegler et al. 2020). These findings, together with the fact that the upper respiratory tract constitutes the primary entry site for the virus, provide a rationale for several of the characteristic clinical manifestations of SARS-CoV-2 infection (3.1.4).

Inside a host cell, the positive-stranded RNA of coronaviruses is often enveloped by a replication organelle which is thought to offer an adequate microenvironment for viral replication (Snijder et al. 2006). Additionally, these membrane-coated particles are thought to restrict cellular innate immune responses by limiting the interaction between viral RNA and pattern recognition receptors in the cytoplasm of host cells. This mechanism was originally discovered in Hepatitis C Virus, which is also a positive-stranded RNA virus, suggesting it may apply to similar RNA viruses (Neufeldt et al. 2016). After replication and assembly, the new virus particles are released from the infected cell, facilitating viral spread throughout the organism.

Once inside the host organism, a virus encounters many different strategies employed by the immune system to combat pathogens (Murphy und Weaver op. 2017). A large number of different proinflammatory cytokines, acute phase proteins, and various cell types are involved. A crucial aspect of anti-viral immune defense is the formation of antibodies. Antibodies are soluble B-cell receptors that recognize specific regions, so called epitopes, of a pathogen. These epitopes are often located on the surface of a virus, e.g. within the spike protein, but can also include peptides throughout the genome of the virus. Since B-cells can interact with the virus itself, but also with viral fragments presented by antigen-presenting cells, a large variety of different antibodies can be generated. Whether induced by infection, vaccination or administered as a therapeutic preparation, antibodies opsonize the virus or its fragments presented by infected cells, sensitizing them for elimination by the immune system (Parkin und Cohen 2001). During the acute phase of infection, IgM antibodies are produced, which promote opsonization indirectly through complement activation. During the course of the disease, they are replaced by IgG antibodies (Li et al. 2020), which are capable of mediating direct opsonization. If viral epitopes recognized by neutralizing antibodies undergo mutational events, immunity against those virus strains may be compromised. Direct response of a virus to selective pressure, e.g. induced by specific antibodies, is referred to as immune escape.

The opsonization of infected tissues with antibodies causes cell damage through the lysis of those cells. In addition, as mentioned earlier, the immune system can detect viral RNA and respond with secreting proinflammatory cytokines. This cytokine release, accomplished through the activation of different subgroups of white blood

cells, can lead to clinical symptoms of the infection. If this pathway is overstimulated by large amounts of viruses and viral antigens, it can lead to a cytokine storm, posing a serious threat to the host (Hirano und Murakami 2020).

3.4. Symptomatology and clinical outline of COVID-19

While approximately 30% of individuals experience asymptomatic infections (Nishiura et al. 2020), the majority of patients develop symptoms within 4-5 days of exposure to SARS-CoV-2 (Lauer et al. 2020). The most common symptoms include fever, cough and fatigue (Guan et al. 2020; Wang et al. 2020). A minority of infected individuals develop more severe symptoms, such as shortness of breath leading to hypoxemia, which may require treatment. Disease surveillance in the United States of America in 2020 reported that 2% of COVID-19 patients were admitted to an intensive care unit (ICU) (Stokes et al. 2020). One study involving 1300 patients at ICU reported that 99% of them required either invasive or noninvasive respiratory support. While there are no definitive factors that predict a severe course of disease, several risk factors have been identified. These include male sex, frailty and co-morbidities such as hypertension, cardiovascular disease, and hypercholesterolemia (Grasselli et al. 2020).

Hospital admissions associated with COVID-19 often present with several nonspecific clinical signs. These parameters can serve as indicators for diagnosing or testing a patient for the SARS-CoV-2 virus. About 80% of patients show lymphocytopenia on admission (Guan et al. 2020). This phenomenon may be explained by the rapid depletion of mostly T-lymphocytes, which are involved in the clearance of the virus. The severity of the disease appears to correlate with C-reactive protein (CRP) levels, as severely ill patients exhibit significantly higher levels compared to those with milder courses of disease (Ali 2020). Furthermore, X-rays of critically ill individuals show severe progression of pneumonia, which can be confirmed through pathohistological analysis. The lung tissue of affected patients is characterized by compromised endothelium-epithelium barrier, triggered by infiltration of immune cells. This inflammation results in endotheliosis, accompanied by edema, which thickens the

alveolar walls and hinders oxygen transfer into the capillaries. This impaired diffusion capacity then results in shortness of breath or even critical hypoxemia (Xu et al. 2020b).

Not only is lung tissue affected by endotheliosis, but the release of newly synthesized viral particles from host cells also leads to direct damage to the endothelium throughout the body (Perico et al. 2021). Large quantities of inflamed capillary tissue may result in the formation of microthrombi, which could explain the high incidence of thrombotic events in COVID-19 patients. These complications include peripheral venous or arterial thrombosis and also pulmonary embolism (Klok et al. 2020). A study including 183 patients with coronavirus pneumonia suggests that a large portion of deaths associated with SARS-CoV-2 is linked to fulminant activation of coagulation, resulting in single or multiple organ failure (Tang et al. 2020).

3.5. Therapeutic strategies

Each course of infection differs from one individual to another, depending on many factors, making it challenging to identify optimal treatment strategies for most patients. Nevertheless, various approaches have emerged, and some therapeutics have shown promising results.

Glucocorticoids are a frequently used group of immunomodulating drugs. They mimic the body's own messenger substance cortisol, but can achieve significantly higher potencies as pharmaceutically produced analogs and are therefore particularly valuable drugs in intensive care medicine. Dexamethasone for example has been shown to significantly reduce the mortality rate in COVID-19 patients requiring respiratory support (Horby et al. 2021).

As described above, COVID-19 is often associated with a cytokine storm, a strong immune response characterized by excessive cytokine secretion and inflammation (Huang et al. 2020). One way to counteract this overshooting immune response is the administration of immunomodulatory agents. Tocilizumab, for example, is an

interleukin-6 receptor inhibitor that has been used to treat patients with critical illness. Data suggests it could be effective in treatment, as it reduces clinical symptoms caused by inflammation as well as hypoxemia (Xu et al. 2020a), confirmed in a randomized, controlled, open-label, platform trial (RECOVERY Collaborative Group 2021).

A different therapeutic approach, particularly in the early stages of the disease, is to block viral replication itself. This can be achieved with replicase inhibitors such as Remdesivir. The drug inhibits the polymerase responsible for replicating viral RNA, resulting in the production of fewer viral particles. It has been proven to shorten the recovery time of treated patients compared to those in the placebo group (Beigel et al. 2020).

To bridge the time until antibodies are produced that neutralize virions and prevent further infection of cells, another therapeutic strategy is to treat naïve patients with convalescent plasma. Clinical data shows that the administration of antibodies effectively terminated periods of viremia in monitored patients (Duan et al. 2020). As an alternative to convalescent plasma, which has limited availability and is difficult to standardize (Hähnel et al. 2020), monoclonal antibodies serve a similar purpose, but can be produced in large defined quantities and thus are more likely to meet clinical requirements. The combination of neutralizing antibodies Casirivimab and Imdevimab has been shown to reduce viral load, symptoms and risk of adverse events associated with COVID-19 in comparison to placebo (Weinreich et al. 2021). Notably, these effects were significant regardless of whether the patient was positive for SARS-CoV-2 antibodies before treatment or not.

Apart from administering different kinds of drugs, several other strategies are now commonly used in COVID-19 therapy within ICUs. One such strategy is positioning patients in prone position. By shifting ventilation in the lung tissue, this treatment quickly ameliorates blood oxygenation and is thus often used in SARS-CoV-2 infected patients requiring oxygen supplementation (Coppo et al. 2020). If prone position does not provide sufficient improvement, a more drastic procedure often taken during this pandemic is to initiate veno-venous extracorporeal membrane oxygenation (VV-ECMO). Though invasive, it is required if adequate pulmonary gas exchange cannot be obtained otherwise. This treatment has been shown to improve outcomes, particularly in younger patients (Kieninger et al. 2023).

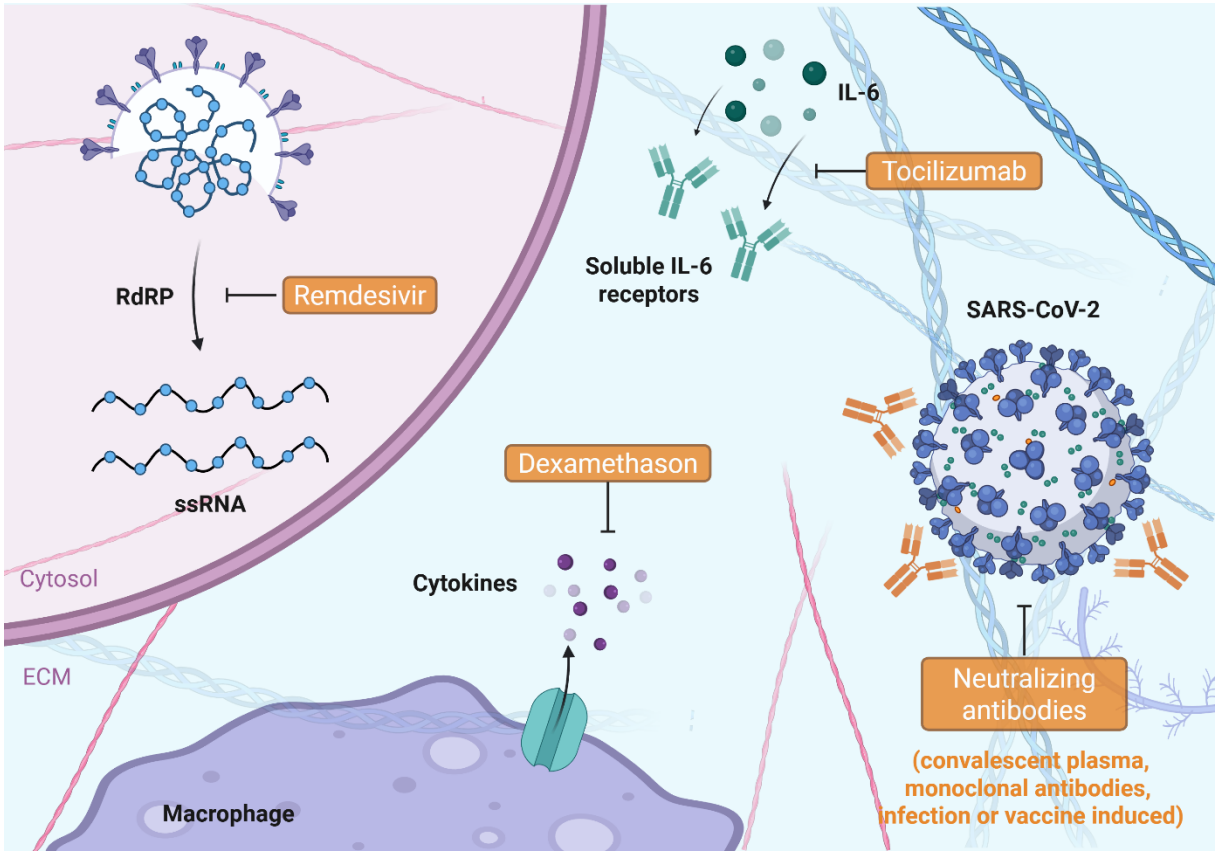


***Figure 2 Therapeutic targets and strategies to treat SARS-CoV-2 infection**. Viral infection and spread is targeted through various mechanisms, interfering with viral replication and neutralizing the virions via administration of antibodies. Additionally, systemic inflammation is addressed by using immunomodulatory drugs. ECM, extracellular matrix; RdRP, RNA-dependent RNA polymerase; IL-6, interleukin 6. Modified from (Hu et al. 2021) and created with BioRender.com.*

In addition to treating infections with SARS-CoV-2, a large field of interest is primary prevention, which focuses on preventing infections from occurring in the first place. As of January 17th 2026, a total of 382 vaccine candidates has been developed worldwide (World Health Organization, COVID-19 vaccine tracker 2026, last accessed on January 17th 2026). Although effective, antibody titers induced by vaccination were found to decrease at 4 months after vaccination (Jo et al. 2021), which might lower effectiveness against acute infection later on. Vaccine development also resembles a race against time, since newly emerging SARS-CoV-2 variants (see 3.6) pose the risk of evading antibodies that have been shown to neutralize previous variants (Iketani et al. 2022). Therefore, achieving population-wide immunity, whether through vaccination or infection, must be accompanied by preventive behaviors at both an individual and social level to contain the spread of the virus as effectively as possible.

3.6. Evolution of SARS-CoV-2 – VOCs

Since the beginning of its spread, SARS-CoV-2 has been constantly evolving, resulting in numerous subvariants circulating worldwide. These new variants are classified as variants of interest (VOI) or variants of concern (VOC) by the World Health Organization (WHO). While VOIs contain genomic alterations which could be associated with increased transmissibility or virulence, VOCs are characterized by their ability to escape previously generated or administered antibodies from infection or vaccination, leading to a higher potential for reinfection and an increased risk of disease severity.

The first alteration of the Wuhan-1 reference genome to achieve global predominance was the D614G amino acid exchange located in the receptor binding domain of the spike protein. It rapidly spread from Europe to the rest of the world, reaching a global dominance of 78% by May 18, 2020 (Korber et al. 2020). Compared to the wildtype reference strain, the D614G variant is associated with increased viral loads (Lorenzo-Redondo et al. 2020).

At that time, SARS-CoV-2 was believed to have a relatively low mutational rate, since the role of nsp14 as the proofreading protein during virion replication within the Coronaviridae had already been discovered in 2006 (Minskaia et al. 2006). However, statistical analysis later revealed a mutational rate of 0.44 mutations a week, leading to approximately two new mutations each month (Amicone et al. 2022). The enforcement of favorable mutations through natural selection has led to the emergence of new mutations within the genome. To simplify communication about emerging lineages and avoid public confusion caused by scientific nomenclature, the WHO virus evolution working group has recommended Greek letters as names for new variants.

In the following section, we focus on the variants of concern (VOCs) pertinent to this study.

In December 2020, the United Kingdom reported the emergence of the Alpha variant (lineage B.1.1.7) as their predominant variant (Leung et al. 2021; Gu et al. 2020). From there, it spread around the globe. This variant carries 17 mutations compared to the Wuhan-1 wildtype, eight of which are located within the spike protein (Davies et al.

2021). One of these spike mutations, the N501Y amino acid exchange, was found to improve the affinity of SARS-CoV-2 to the ACE2 receptor located on host cell membranes (Gu et al. 2020), improving viral fitness. Furthermore, studies showed decreased efficiency of neutralizing antibodies (generated artificially or triggered upon infection or vaccination) against VOC Alpha (Chen et al. 2021). The risk for reinfection was not thought to be higher than the one for the wildtype, and initial symptomatology did not differ considerably (Graham et al. 2021). However, large observation studies showed an increased risk for admission to critical care units and mortality compared to patients infected with other lineages (Patone et al. 2021).

The situation evolved further when the Delta variant, designated as lineage B.1.617.2, was declared a VOC in May 2021. It was first reported in India, carrying the E484Q and L452R mutations, which set it apart from the other variants (Choudhary et al. 2021). Especially the L452R mutation enhanced the virus's fitness by stabilizing the binding of the spike protein to the ACE2 receptor, thereby increasing its infectivity (Deng et al. 2021). To the concern of the public health systems, VOC Delta was found to be even more closely associated with severe disease progression and death than earlier variants (Ong et al. 2022). One specific mutation, the P323L located within the polymerase of the virus, predominantly occurred in severe courses of infection (Biswas und Mudi 2020). It increases the speed of replication and is therefore suspected to weaken proof-reading efficacy and thus to be responsible for an increased mutation rate (Alam et al. 2022). This effect may also be linked to its decreased sensitivity towards antibodies. An *in vitro* study found VOC Delta to be six times less sensitive to convalescent serum and eight times less sensitive to vaccine-elicited antibodies, compared to the D614G variant (Mlcochova et al. 2021).

3.7. Aim and objectives

Our aim was to contribute to the understanding of SARS-CoV-2 evolution *in vivo* and identify factors driving viral adaptation. We therefore monitored viral evolution within hospitalized patients at the University Hospital Regensburg. Identifying the factors that promote viral genomic changes throughout the course of the infection is crucial for more effective individual treatment of COVID-19 patients in regards to the emergence and prevention of new, potentially more pathogenic, mutations.

In total, we analyzed clinical and virological data from 27 patients. To improve the validity and statistical power of our observations, we also included data from 16 additional patients obtained from similar analysis conducted as part of the master thesis of Clara Luzia Magnus. By comparing patient cases infected with the Wuhan-1 wild type strain as well as VOCs Alpha and Delta, we aimed to increase the predictive power of our results for newly emerging subtypes. As the duration of viral replication had already been shown to be associated with increased probability of genome alterations in earlier work by the study group (Magnus et al. 2022), patients were pre-selected based on prolonged infection.

Through next generation sequencing genome analysis, we aimed to identify mutational hotspots. Statistical analysis was subsequently used to identify factors which are shared by all patients with genome alterations. Based on our results we discuss possible explanations for the occurrence of mutations and the significance of determined risk factors and compare them to the current state of scientifical knowledge.

To take a closer look on the role and dynamics antibodies play in *in vivo* evolution, we measured antibody activity against SARS-CoV-2 wildtype spike and nucleocapsid protein, comparing sera collected from patient who developed amino acid exchanges, comparing reactivity before and after the emergence of genomic alterations.

4. Material and Methods

4.1. Material

Consumables	Manufacturer, catalogue no.
Gloves Peha-soft-nitrile FINO	Paul Hartmann AG, Heidenheim (DE), 942196
Pipette tips, 10 µl, 100 µl, 1000µl	Eppendorf AG, Hamburg (DE), P12992B, P13871B, P14685B
Pipette tips, filter tip, 20 µl	Sarstedt AG & Co. KG, Nümbrecht (DE), 70.3020.355
Reaction tubes, 0.5 ml	Sarstedt AG & Co. KG, Nümbrecht (DE), 72.699
Reaction tubes, 1.5 ml	Eppendorf AG, Hamburg (DE), 0030125150
Reaction tubes, 2 ml	Greiner Bio-One GmbH, Frickenhausen (DE), 623 201
SafeSeal SurPhob sterile pipette tips, 100 µl, 300 µl	Biozym, Hessisch Oldendorf (DE), VT0230, VT0250
Tubes, 15 ml, 50ml	Sarstedt AG & Co. KG, Nümbrecht (DE), 62.554.502, 62.547.254
PCR Reagents	Manufacturer, catalogue no.
SARS-CoV-2 E _Sarbeco_F1	Metabion international, Planegg (DE), N/A
SARS-CoV-2 E _Sarbeco_F2	Metabion international, Planegg (DE), N/A
SARS-CoV-2 E _Sarbeco_P1	Metabion international, Planegg (DE), N/A
Taq-Path-Mix	Metabion international, Planegg (DE), N/A
Commercial Kits	Manufacturer, catalogue no.
PCR	
EZ1 DSP Virus Kit	QIAGEN, Hilden (DE), 62724
MicroAmp Fast Optical 96-Well Reaction Plate with Barcode (0.1ml), MicroAmp Optical 8-Cap Strip	Applied Biosystems by Life Technologies/ThermoFisher Scientific, Darmstadt (DE), 4346906, 4323032

Peptide Microarray	Manufacturer, catalogue no.
Goat anti-Human antibodies	Goat anti-Human IgG Fc Cross-Adsorbed Secondary Antibody, DyLight 680, Invitrogen Life Technologies GmbH, Darmstadt (DE), SA5-10138
Incubation Tray 3/4	PEPperPRINT GmbH, Heidelberg (DE)
Mouse control antibodies	Mouse Monoclonal anti-HA (12CA5)-DyLight800 Control Antibody, PEPperPRINT GmbH, Heidelberg (DE), Batch 0921
PEPperCHIP® Custom Peptide Microarray, Spike (UniProt ID: P0DTC2, 1273 aa), Nucleocapsid (UniProt ID: P0DTC9, 419 aa), customized	PEPperPRINT GmbH, Heidelberg (DE)
Rockland Blocking Buffer	PEPperPRINT GmbH, Heidelberg (DE), MB-070
Next Generation Sequencing	Manufacturer, catalogue no.
Ion AmpliSeq™ SARS-CoV-2 Research Panel	Thermo Fisher Scientific, Massachusetts (US), A51306
IonTorrent™ Genestudio S5 Plus instrument	Thermo Fisher Scientific, Massachusetts (US), A38195
Devices	Manufacturer, catalogue no.
Centrifuge Rotina 380R	Hettich, Tuttlingen (DE), 1701
Eppendorf Research Plus	Eppendorf AG, Hamburg (DE), N/A
EZ1 Advanced XL platform	Qiagen, Hilden, DE, 9001875
Freezing Container	Mr. Frosty, Thermo Fisher Scientific, Massachussetts (US), 5100-0001
Laminar Flow	BDK Luft- und Reinraumtechnik GmbH, Sonnenbühl-Genkingen (DE), EN 12469
Pipetus	Hirschmann Laborgeräte GmbH & Co. KG, Eberstadt (DE), 81211095
StepOnePlus Realtime PCR System	Thermo Fisher Scientific, Schwerte, (DE), 4376600
Vortex-genie 2	Scientific Industries, New York (US), SI-0236
Software	Manufacturer

GraphPad Prism	GraphPad Software, version 9.1.2.226 for Windows, California (US)
IBM SPSS Statistics	Version 28, IBM Deutschland GmbH, Ehningen (DE)
MAPIX Analyzer	PEPperPRINT Print GmbH, Heidelberg (DE)

4.1.1. SARS-CoV-2 oligonucleotides

Oligonucleotide	Target gene	Sequence	Working Concentration
E_Sarbeco_F1	SARS-CoV-2 E gene	5' ACAGGTACGTTAATAGTTAATAGCGT 3'	400nM
E_Sarbeco_R2	SARS-CoV-2 E gene	5' ATATTGCAGCAGTACGCACACA 3'	400nM
E_Sarbeco_P1	SARS-CoV-2 E gene	5' FAM-ACACTAGCCATCCTTACTGCGCTTCG-BBQ 3'	200nM

4.2. Methods

4.2.1. Molecular biology

4.2.1.1. SARS-CoV-2 RNA isolation and RT-qPCR testing

To measure the viral load in patient samples selected for further analysis, RNA was extracted using the EZ1 DSP Virus Kit (QIAGEN, Hilden, DE) on the EZ1 Advanced XL platform (QIAGEN, Hilden, DE), yielding 100µl of RNA eluate for further processing. The SARS-CoV-2 envelope gene was amplified using the TaqPath Mix on the StepOnePlus Real-Time polymerase chain reaction (PCR) System (Thermo Fisher Scientific, Schwerte, DE) following a published protocol (Corman et al. 2020). Assay-specific RNA standards were used to quantify the SARS-CoV-2 RNA (Hitzenbichler et al. 2021).

Table 1 SARS-CoV-2 quantitative RT-qPCR protocol

Step	Cycles	Temp. [C°]	Time [min]
cDNA synthesis	1	50	15:00
Reverse transcriptase inactivation and Taq-polymerase activation	1	95	02:00
Denaturation	45	95	00:05
Annealing and extension	45	60	00:30

4.2.1.2. Next generation sequencing

The extracted RNA was submitted to Dr. Andreas Hiergeist, a specialist in next-generation sequencing (NGS) at the Institute of Clinical Microbiology and Hygiene, University Hospital Regensburg, for library preparation and downstream analysis. To ensure adherence to strict quality criteria, the inhouse standard protocol was closely followed as described previously (Magnus et al. 2022). In brief, the Ion AmpliSeq™ SARS-CoV-2 Research Panel (Thermo Fisher Scientific, Massachusetts, US) was used to perform PCR-based whole genome sequencing. For this purpose, the purified virus genome was fragmented and then amplified based on the viral load. The amplicons in the panel cover >99% of the SARS-CoV-2 genome as well as human expression controls. The resulting pool of viral copies was quantified again using real-time PCR. The IonTorrent™ Genestudio S5 Plus instrument (Thermo Fisher Scientific, Massachusetts, US), a high throughput system used for validation of sequencing libraries, facilitated rapid quality control. Results were analyzed with the SARS-CoV-2 Research Plug-in Package. The cut-off for successful sequencing was set as a mean genome coverage above 1,000-fold. Each genome was mapped to the Wuhan-Hu-1 sequence (GenBank acc. no. MN908947), serving as reference genome to detect single nucleotide polymorphisms. Raw sequencing reads were mapped to the SARS-CoV-2 reference genome (NC_045512.2) using Bowtie2 (v2.5) (Langmead und Salzberg 2012). The resulting BAM files were sorted and indexed with samtools. Variant calling was performed using LoFreq (v2.1.5) (Wilm et al. 2012), applying indel quality recalibration and a minimum coverage threshold of 10× per site. Variants were

filtered using an allele frequency threshold of 0.1% with a minimum read depth of 20 to enable low-frequency variant detection. For functional annotation, all VCF files were processed with SnpEff (v5.2) (Cingolani et al. 2012) to classify variant effects and amino acid changes at each site, using a custom database built from the reference FASTA file and a curated GFF3 annotation describing all SARS-CoV-2 genes and non-structural proteins.

4.2.1.3. Genome sequence analysis

Whole viral genomes were analyzed and taxonomically classified using the open source repositories from Stanford University (Tzou et al. 2022) and GISAID (Khare et al. 2021). These systems compare submitted data to the Wuhan-Hu-1 sequence, the first published SARS-CoV-2 genome, and highlight discrepancies. The sample to be analyzed can thus be taxonomically categorized based on its specific genomic alterations, as certain mutations characterize the different SARS-CoV-2 variants-of-concern.

4.2.2. Clinical data assembly

Clinical data for each patient were collected retrospectively in collaboration with the treating physicians from the intensive care units at the University Hospital Regensburg. We focused on multiple factors as possible variables that might influence the emergence of SARS-CoV-2 mutations. Some variables were defined by the patient and his or her medical history (age, gender, time between samples used for analysis, virus variant of infection, BMI, SARS-CoV-2 vaccination status, blood type and previously diagnosed conditions such as chronic obstructive pulmonary disease (COPD), arterial hypertension, diabetes, organ transplantation or nicotine abuse). Other parameters describe the virological course of infection (IgG antibodies at

hospitalization and discharge, as well as viremia) and chemical laboratory test results (d-dimers, CRP at hospitalization, leucocyte and lymphocyte cell counts). We also collected data on the patient's condition at hospitalization (sequential organ failure assessment (SOFA) score, need for catecholamines, body temperature), clinical treatment strategies (administration of convalescent plasma, immunosuppressive drugs, Remdesivir, monoclonal antibodies) over the course of the disease and outcomes (ICU duration, need for prone positioning, extracorporeal membrane oxygenation (ECMO) duration, dialysis, thrombosis, concomitant viral, bacterial or fungal infection, outcomes of the patient).

4.2.3. COVUR study

4.2.3.1. Ethical Statement and funding

The ethical commission at the Faculty of Medicine (Ref. no. 20-1785-101), University of Regensburg, approved the collection of clinical specimens as part of the COVUR study. The Bavarian Ministry of Science and Art funded the project.

4.2.3.2. Sample collecting and sample sorting

To gather information about SARS-CoV-2 evolution *in vivo*, we selected 27 patients from the COVUR study who were hospitalized at the ICU of the University Hospital Regensburg between November 2020 and December 2022. These patients were selected for preferably long periods of infection with SARS-CoV-2, since prior studies of the group had suggested a link between the duration of viral replication and the occurrence of mutations. Additionally, two or more IgG antibody tests during the course of the disease were required in order to map B-cell immune response via antibody levels during the infection.

During hospitalization, nasopharyngeal swabs, gargle samples, bronchoalveolar lavage fluid (BAL), and tracheal aspirates were collected as part of the routine clinical monitoring of the patients. A cutoff of 10^3 SARS-CoV-2 RNA copies/ml was established to ensure success of next generation sequencing. Patient samples were stored at -80°C to ensure RNA stability before processing.

4.2.4. SARS-CoV-2 PEPperChip peptide microarray

To explore SARS-CoV-2 antibody binding patterns and their dynamics with occurring genome alterations, we analyzed pre- and post-alteration serum samples of patients with such alterations in the spike and nucleocapsid protein, using the customized PEPperChip Peptide Microarray Immunoassay (PEPperPRINT GmbH, Heidelberg, DE). It covers the full-length sequence of both proteins with 15-mer overlapping peptides (Spike: UniProt ID: P0DTC2, 1273 aa, Nucleocapsid: UniProt ID: P0DTC9, 419 aa), allowing specific testing for each epitope. All patients with genomic alterations in these proteins were identified through genome sequence analysis, as described above.

First, the incubation tray was cleaned and assembled, followed by incubation at 21°C with washing buffer and Rockland blocking buffer. Next, the arrays were incubated in the dark at 21°C for 45 minutes with a goat anti-human IgG Fc Cross-Adsorbed DyLight 680 secondary antibody (Invitrogen, Carlsbad, USA), using a 1:100 dilution in staining buffer. Arrays were washed and air-dried, then scanned at 700 and 800nm to detect fluorescence from the secondary antibodies that were non-specifically bound to the peptides.

After re-incubating at 21°C the arrays with staining buffer, patient sera were diluted 1:1000 with staining buffer and incubated overnight at 4°C on an orbital shaker with 100 rpm. The next day the arrays were washed to remove residual non-specifically or unbound antibodies and other serum compounds, thereby reducing background noise. This was followed by incubation with the secondary antibody and scanning, as described above.

Lastly, the incubation, washing, and scanning steps were repeated with the mouse anti-HA (hemagglutinin) control antibody (12CA5)-DyLight800 (PEPperPRINT), using a 1:2000 dilution with staining buffer.

To interpret the results, the background scan obtained before adding patient sera was subtracted from the final scan. The number of attached antibodies correlates with the intensity of the detected immunofluorescent signals at each spot. MAPIX software for microarray image analysis and data quantification (PEPperPRINT GmbH, Heidelberg, DE) was utilized to analyze the generated data.

4.2.5. Statistical analysis, graph compilation and use of translation tools

IBM SPSS Statistics™ 28 was used to conduct statistical analysis for this project. We used two-sided statistical tests, and p-values <0.05 and $p<0.01$ were considered significant and highly significant, respectively. To determine the factors driving amino acid exchanges in the SARS-CoV-2 genome, we compared the group of patients with genomic alterations between the first and second samples to the group of patients without genomic changes (variables called ´change´ and ´no change´). Comparisons were performed using binary logistic regression models for all investigated parameters. Parameters that showed significant differences between the two groups were checked for multicollinearity using Spearman´s correlation coefficient. Multivariate binary logistic regression was performed using both forward and backward modeling approaches. We report odds ratios and respective 95% confidence intervals along with p values of all investigated parameters in table 4.

Figures were compiled using GraphPad Prism (version 9.1.2.226 for Windows, GraphPad Software, California, US) and illustrations were created using BioRender. The ladder provides building kits partly incorporated into illustrations designed for this work.

The translation tool DeepL was solely used to compare differences in terminology between German and English in order to find the best possible wording.

5. Results - Study of SARS-CoV-2 evolution *in vivo*

5.1. Clinical characteristics of the patient cohort at hospital admission

In this study, we took a closer look at several variables from patients who were hospitalized at the University Hospital Regensburg between 2020 to 2022 due to severe SARS-CoV-2 infection. Overall, we selected 43 patients, two of which had to be excluded because of an insufficient amount of viral load below the cut off to ensure reliable genome analysis. Out of these 43 patients, 16 had already been included in a next generation sequencing study, performed by Clara Luzia Magnus, who published the results in her Master thesis (Evolution of SARS-CoV-2 under selection pressure 2021). All of the selected patients gave their consent in the framework of the COVUR study, which was approved by the ethical commission of the Faculty for Medicine, University of Regensburg (Ref. no. 20-1785-101).

As one of our aims was to identify parameters that influence the occurrence of mutational events over the course of the SARS-CoV-2 infection, we first examined variables determined by the patient and the condition with which the patient was admitted to the hospital. Statistical analysis of each parameter in relation to mutational events can be found in chapter 9.1. Among the 41 patients enrolled in the study, 25 were male. (**Fig. 3A**). The age ranged from 23 to 81, with a median of 63.0 years (**Fig. 3B**). The body mass index (BMI) showed a relatively even distribution across normal range values (BMI 18.5-24.9), overweight (25-29.9), and obesity classes I (30-34.9), II (35-39.9) and III (40 and above) (**Fig. 3C**).

Blood type distribution was as follows: 0 Rhesus factor positive (Rh pos) 42.1%, A Rh positive 28.9%, B Rh positive 2.6%, AB Rh positive and 0 Rh negative (Rh neg) each 7.8%, and A negative as well as B negative, each 5.2% (**Fig. 3D**). The blood group distribution in our cohort was fairly representative of the general population in Germany, although type 0 Rh positive accounts for only about 35% and type A Rh positive for approximately 37% of the population (Statista 2020, last accessed on January 17th 2026). The vaccination status was known for only 23 patients, of whom two had received at least one dose of COVID-19 vaccine (**Fig. 3E**). These numbers

have to be seen in a temporal context, as most patients contracted SARS-CoV-2 early in the pandemic, when no vaccine was yet available.

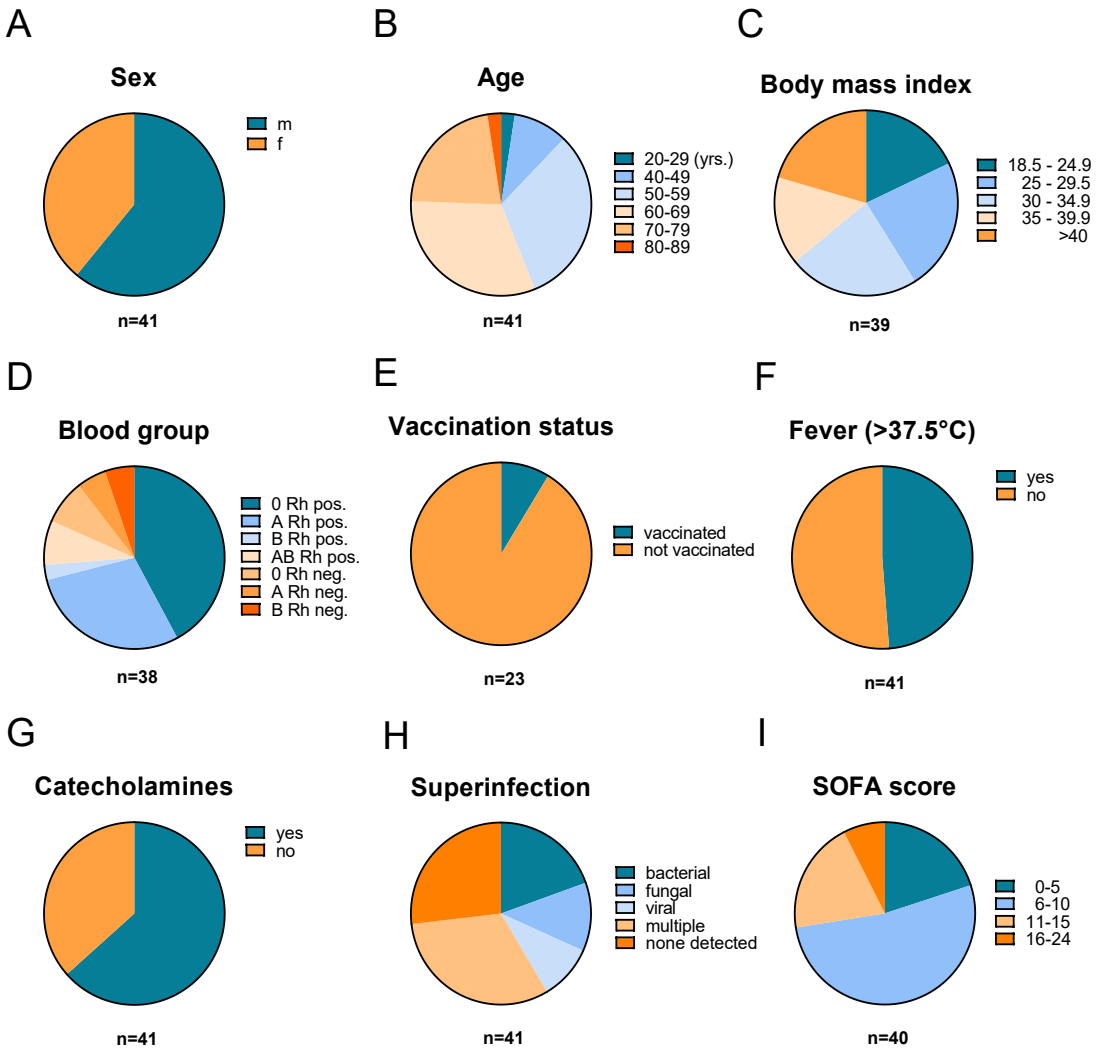


Figure 3 Clinical characteristics of the patient cohort at admission to the intensive care unit (ICU). Description of the patient cohort (n=41) with available information on (A) sex, (B) age, (C) body mass index, (D) blood group, (E) SARS-CoV-2 vaccination status, (F) fever, defined as body temperature exceeding 37.5 degrees Celsius, (G) administration of catecholamines, (H) superinfection, defined as an infection caused by any viruses, bacteria or fungi concurrent with the SARS-CoV-2 infection, and (I) SOFA Score. Patients with incomplete data on the specified parameters were excluded from the analysis. F, female; m, male; n, number of included patients; neg., negative; pos., positive; Rh, Rhesus factor; SOFA, sequential organ failure assessment; yrs., years, reproduced from (Kraft et al. 2026).

On admission roughly half of the cohort (48.7%) presented with fever, defined as a body temperature exceeding 37.5° Celsius (**Fig. 3F**). Additionally, 63.4% (n = 26)

needed circulatory assistance through the administration of catecholamines (**Fig. 3G**). Furthermore, only 11 patients had no other infection besides SARS-CoV-2, while 8 patients had additional bacterial infection, 5 fungal infections, 4 viral infections and 13 patients (31.7%) were infected with multiple other pathogens (**Fig. 3H**). Lastly, we recorded the SOFA score for each patient. It summarizes the functionality of the respiratory tract, circulatory system, central nervous system, coagulation process as well as liver and kidney function. While clinical conclusions can only be drawn from this score when the score of an individual rises, it does give an overall impression of the patients' condition, stating that only 20% of our cohort had a value between 0 to 5 points and thus acceptable organ function (**Fig. 3I**).

5.2. Laboratory parameters at admission of the patients

We also collected various blood parameters upon admission to ICU, as they provide a first indication of how the disease might progress in each individual. D-dimers point to an activated coagulation and often reflect recent minor or major thrombotic events. Only two patients from our cohort showed physiological values (≤0.5 µg/ml), while the majority (n = 20) showed elevated (between 0.5-3.9 µg/ml), or even strongly elevated values (n = 17, >4 µg/ml), with a median of 3.0 µg/ml (**Fig. 4A**). CRP (C-reactive protein), an inflammatory marker, was elevated in all patients (>5 mg/l), even strongly elevated in the vast majority (n = 28, 5.1-100 mg/l), with a median of 153 mg/l, indicating systemic inflammation (**Fig. 4B**). The leukocytes were reduced (<4 cells $x10^3$/µl) in two patients, and elevated (>9 cells $x10^3$/µl) in 23 patients with a median of 10.9 $x10^3$/µl (**Fig. 4C**). Moreover, most patients (n = 28) showed a lymphocytopenia (<1.18 cells $x10^3$/µl), while the remaining patients (n = 12) had lymphocyte counts at the lower end of the physiological range (1.18 – 3.74 cells $x10^3$/µl), with a median of 0.81 $x10^3$/µl (**Fig. 4D**). These numbers point to a shortage of lymphocytes due to an increased consumption through an activated immune response towards the virus. Additionally, certain immunosuppression used in treatment for patients included in our study (see 5.3, Cyclophosphamide and Tacrolimus) induce cell death and hinder

proliferation as their mechanism of action and therefore further enhance lymphocytopenia. The yet displayed overall leukocytosis in the majority of our cohort can thus be explained by a reactive overcompensation of other subgroups of leukocytes, mainly neutrophils.

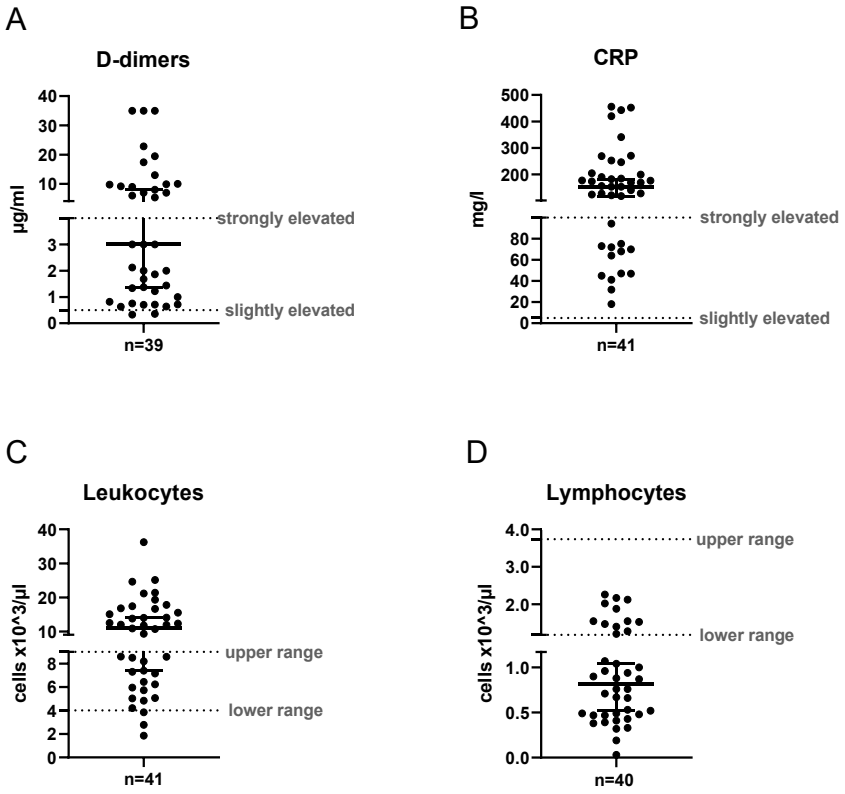


Figure 4 Laboratory parameters at admission of the patient cohort to the intensive care unit (ICU). After admission, blood samples were collected from each patient. The graphs illustrate the first specimens collected for (A) D-dimers (a marker for thrombotic events), (B) CRP (an inflammatory marker), (C) leukocytes and (D) lymphocytes (immune defense cells). Lower dotted lines indicate thresholds for slightly elevated values (A, B) and lower range of physiological values (C, D), upper dotted lines indicate thresholds for strongly elevated values (A, B) and upper range of physiological values (C, D). Cells x10^3/µl, cells times 10^3 per microliter; CRP, C-reactive protein; µg/ml, microgram per milliliter; mg/l, milligram per liter; n, number of included patients, reproduced from (Kraft et al. 2026).

5.3. Clinical follow-up of the patients upon treatment

Since each course of infection is influenced by the medical history summarizing the constitution of the individual prior to infection, we also collected data regarding known conditions, such as heart transplantation (n = 2), diabetes (n = 12), hypertension (n = 20) and COPD (n = 4) (**Fig. 4A**).

Furthermore, different therapy strategies can influence viral replication and thus the emergence of new mutations. Much of our current understanding of intra-host SARS-CoV-2 evolution stems from studies involving severely immunocompromised individuals. Notably, the Δ69/Δ70 deletion in the spike protein was first identified in such a patient (Kemp et al. 2021), prior to becoming a hallmark of the Alpha variant. We therefore recorded the number of patients who were treated with any kind of immunosuppression (including different kinds of glucocorticoids (Hydrocortisone, Prednisolone, Betamethasone, Dexamethasone), Cyclophosphamide and the IL-6 antibody inhibitor Tocilizumab, n = 34), Remdesivir (n = 13), monoclonal antibodies (n = 5), convalescent plasma (n = 19), prone position bedding maneuver (n = 23) and extra-corporal membrane oxygenation (ECMO, n = 16) (**Fig. 4B**). Additionally, 11 patients developed thrombosis, 16 patients needed temporal dialysis due to acute renal insufficiency, and sadly, 14 patients deceased while on the ICU (**Fig. 4C**).

We also monitored the time, measured in days, which patients spent in the ICU (**Fig. 4D**), and on ECMO (**Fig. 4E**). The median ICU stay was 30 days, ranging from 6 to 112 days, while the median duration of ECMO therapy, calculated for all patients who did receive this treatment, was 21 days, ranging from 2 to 93 days.

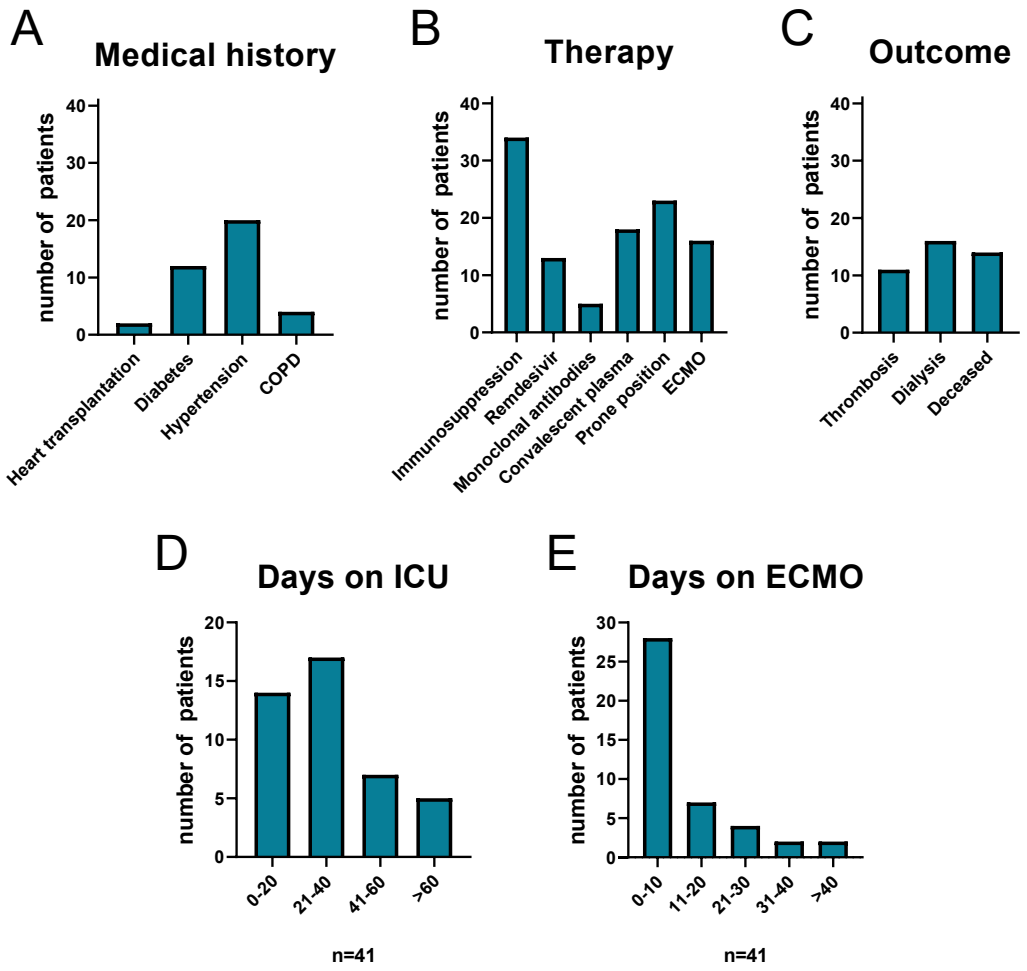
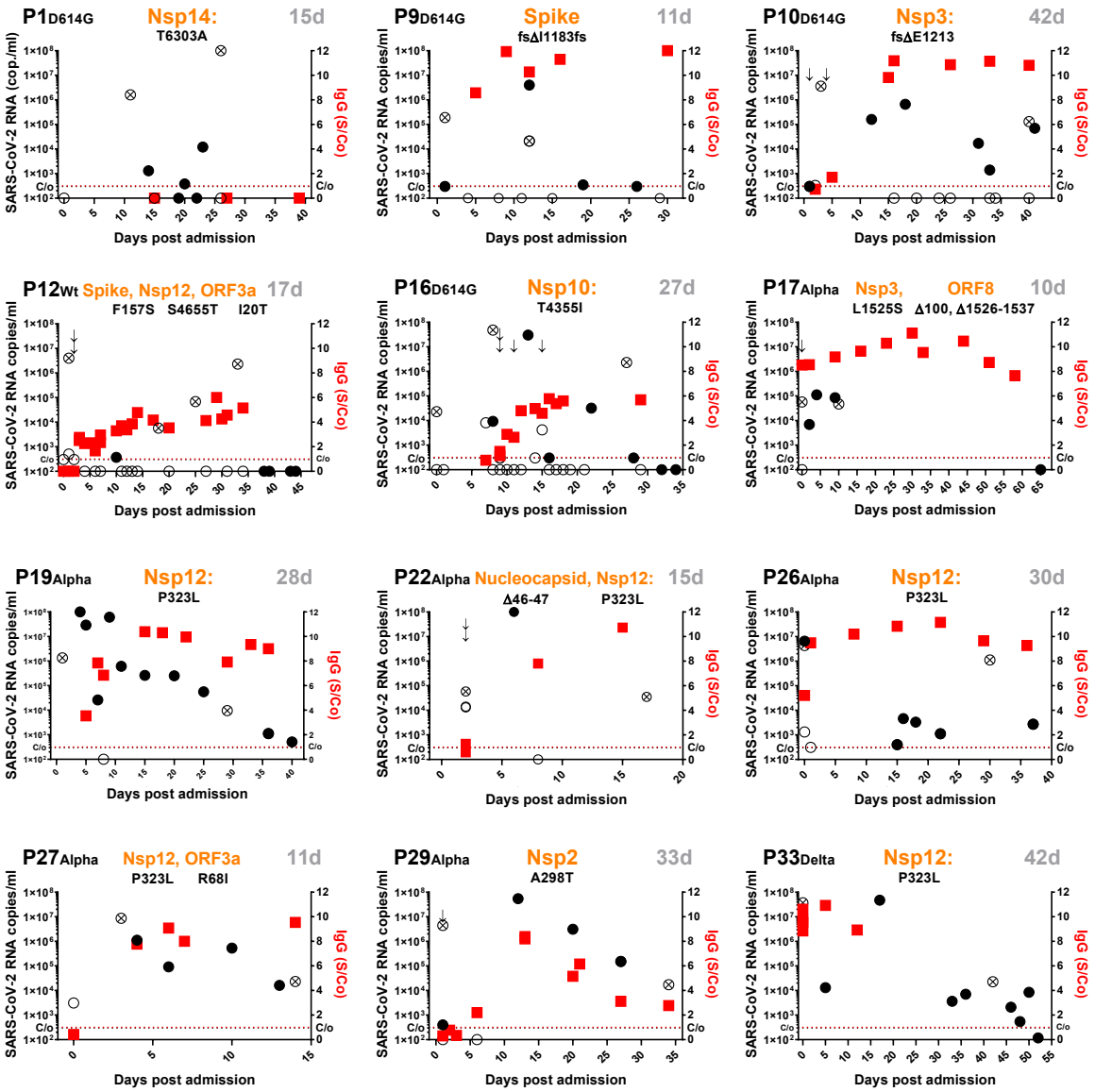


Figure 5 Pre-existing conditions, treatments and outcomes of SARS-CoV-2 infection. Bar graphs illustrating (A) the medical history of the patient cohort, (B) individual therapy strategies, (C) treatment outcomes, (D) days spent on ICU and (E) ECMO. COPD, chronic obstructive pulmonary disease; ECMO, extracorporeal membrane oxygenation; ICU, intensive care unit; n, number of included patients, reproduced from (Kraft et al. 2026).

5.4. Disease progression based on virological parameters shows an inverse correlation between viral load and immune response

We monitored 41 patients from the ICU at University Hospital Regensburg with severe COVID-19 infection, focusing on respiratory and serum viral loads as well as SARS-CoV-2 IgG antibody titer levels. Samples analyzed for respiratory viral load included throat swabs, pharyngeal lavage, bronchial secretions and bronchoalveolar lavage specimens. Additionally, we collected information about the administration of convalescent plasma (SARS-CoV-2 IgG antibodies from convalescent donors via plasmapheresis) and referenced NGS analysis results (see chapter 7) above the respective graphs.

In total, we analyzed and plotted SARS-CoV-2 IgG antibody levels from 325 blood samples, as well as viral loads from 121 blood samples and 288 respiratory samples. Each patient's individual course of infection is depicted in the following graphs (**Fig. 6** illustrates the course of disease in patients with genomic alterations between the first and second analyses, while **Fig. 7** shows patients without such alterations).


P1D614G Nsp14: T6303A 15d
P9D614G Spike fsΔI1183fs 11d
P10D614G Nsp3: fsΔE1213 42d
P12Wt Spike, Nsp12, ORF3a F157S S4655T I20T 17d
P16D614G Nsp10: T4355I 27d
P17Alpha Nsp3, L1525S Δ100, Δ1526-1537 ORF8 10d
P19Alpha Nsp12: P323L 28d
P22Alpha Nucleocapsid, Nsp12: Δ46-47 P323L 15d
P26Alpha Nsp12: P323L 30d
P27Alpha Nsp12, ORF3a P323L R68I 11d
P29Alpha Nsp2 A298T 33d
P33Delta Nsp12: P323L 42d
SARS-CoV-2 RNA (cop./ml)
SARS-CoV-2 RNA copies/ml
IgG (S/Co)
C/o
Days post admission

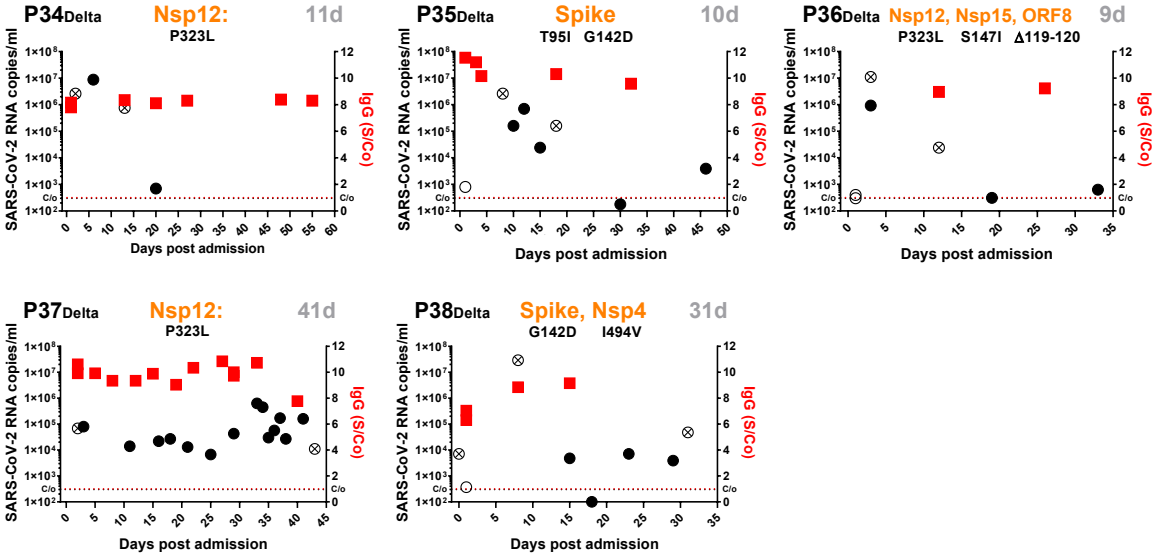
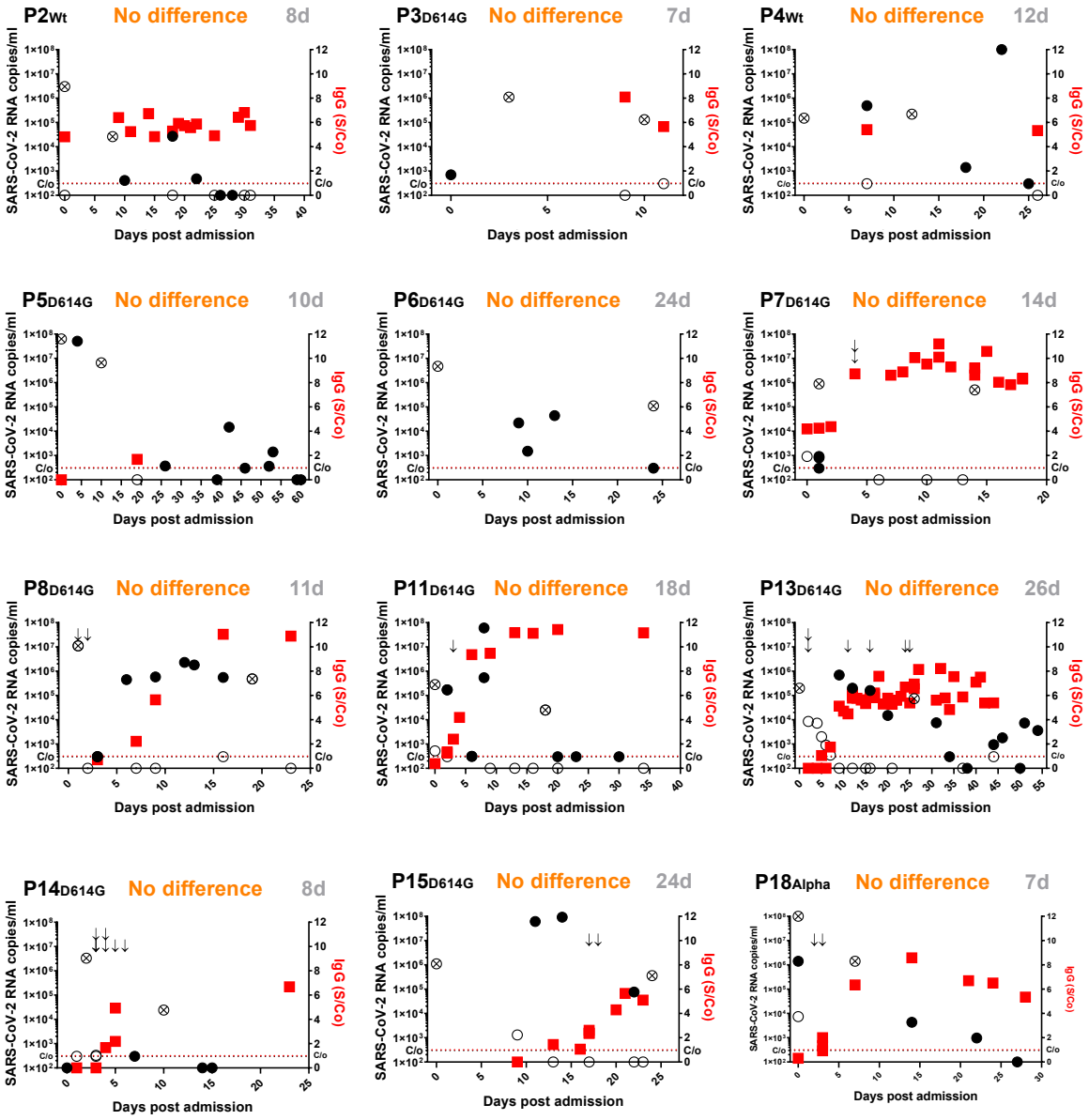
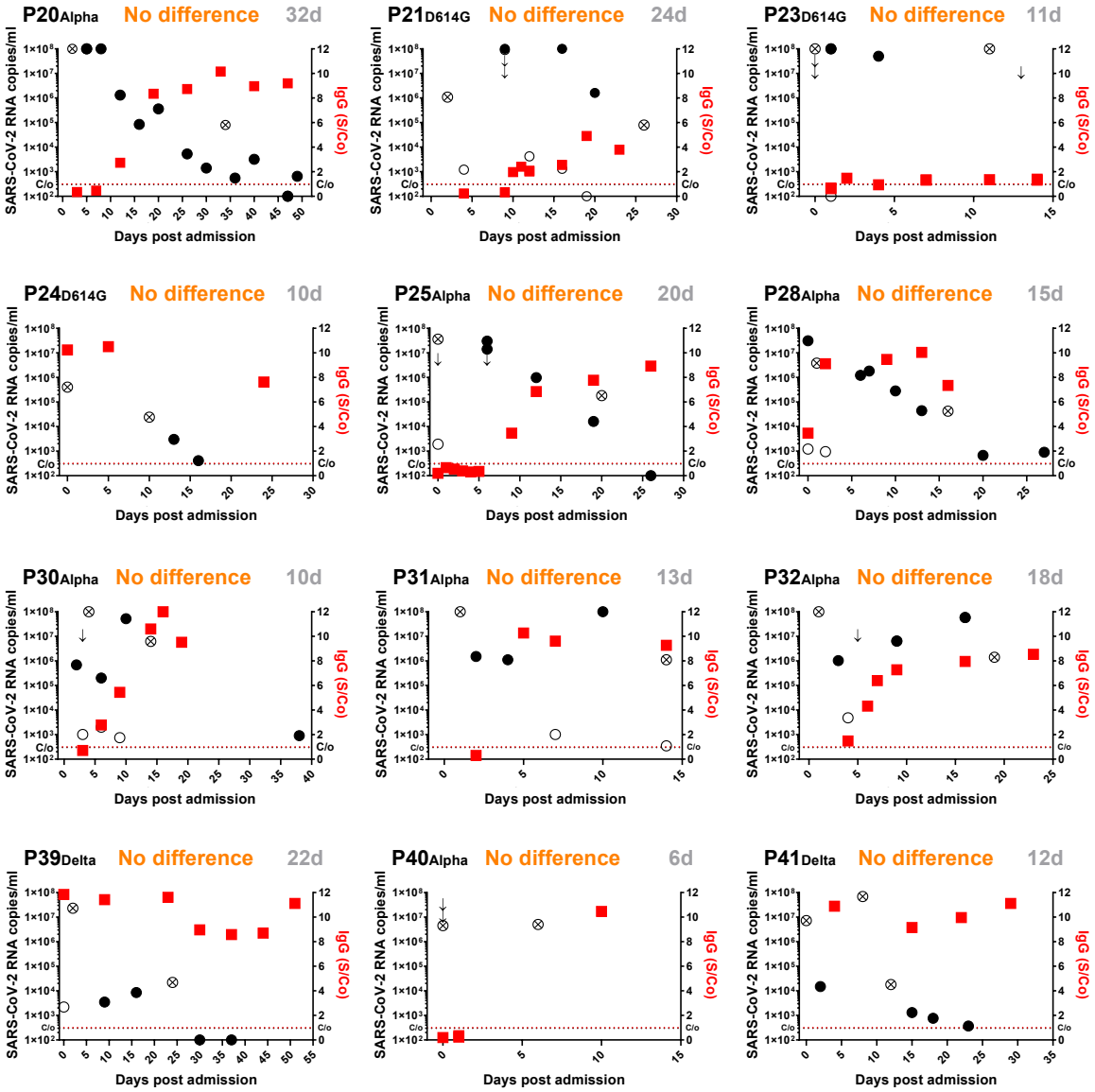


Figure 6+7 Monitoring of COVID-19 disease progression in hospitalized patients with regard to virological parameters. Course of disease in all study patients hospitalized at the University Hospital Regensburg from 2020 to 2022. The full-length viral genome obtained from respiratory samples of patients via next generation sequencing was compared to the Wuhan-1 SARS-CoV-2 reference genome (GenBank acc. no. MN908947). Each graph (1-41) represents one patient. The viral variant is listed next to each patient number in the top left corner as Wuhan-1 Wildtype (wt), European Wildtype (D614G), and variant-of-concern Alpha or Delta. The number of days (d) between the first and second sample used for NGS analysis are shown in grey in the top right corner. Days post hospital admission are depicted on the x-axis. The left y-axis shows the viral load in patient samples as viral copies per milliliter (cop./ml). Samples used for next generation sequencing to screen for new mutations occurring *in vivo* are indicated with marked circles. All other respiratory samples are shown in black circles. Blank circles represent viremic samples. SARS-CoV-2 IgG antibody levels are displayed as red squares on the right y-axis. If mutational events occurred during the course of the disease in individual patients (figure 6), the corresponding gene (underlined) and amino acid exchange and location are listed in orange and black above the respective graph; if no mutational event occurred (figure 7), graph states “no difference”. Black arrows indicate administration of convalescent plasma. Cop., copies; D, days; Δ, amino acid deletion; fs, frame shift mutation; IgG, immunoglobulin G; nsp, non-structural protein; ORF, open reading frame; p, patient; S/Co sample-to-cutoff ratio, reproduced from (Kraft et al. 2026).


P2Wt No difference 8d
P3D614G No difference 7d
P4Wt No difference 12d
P5D614G No difference 10d
P6D614G No difference 24d
P7D614G No difference 14d
P8D614G No difference 11d
P11D614G No difference 18d
P13D614G No difference 26d
P14D614G No difference 8d
P15D614G No difference 24d
P18Alpha No difference 7d
SARS-CoV-2 RNA copies/ml
IgG (S/Co)
Days post admission
C/o


P20Alpha No difference 32d
P21D614G No difference 24d
P23D614G No difference 11d
P24D614G No difference 10d
P25Alpha No difference 20d
P28Alpha No difference 15d
P30Alpha No difference 10d
P31Alpha No difference 13d
P32Alpha No difference 18d
P39Delta No difference 22d
P40Alpha No difference 6d
P41Delta No difference 12d
SARS-CoV-2 RNA copies/ml
IgG (S/Co)
C/o
Days post admission

In our cohort, 51% (n = 21) of the patients were seronegative for SARS-CoV-2 IgG at admission. Over the course of the treatment, 46.3% (n = 19) received at least one dose of convalescent plasma, 13 patients received two or more doses. In total, 44 doses were administered during our period of study. The graphs show a clear rise of SARS-CoV-2 IgG antibody levels after administration of convalescent plasma (**Fig. 6 P10; P12; P16; P17; P22; P29** and **Fig. 7 P7; P8; P11; P13; P14; P15; P18; P21; P23; P25; P30; P32; P40)**, except for patient 23 (**Fig. 7 P23**). Patients who did not receive antibodies as a treatment, managed to develop their own IgGs against the virus. Solely one patient (**Fig. 6 P1**) remained seronegative throughout the entire observation period. Reasons for the atypical course of P1 and P23 are discussed in chapter 6.3.

In summary, viral loads in both blood and respiratory specimens decreased as SARS-CoV-2 IgG antibody levels increased in most patients.

5.5. Virological profile reveals that most patients experienced a viremic phase

At ICU admission, 50% of the cohort had a median viral load of 3.0 x 10^6 cop./ml (interquartile range, 2.4 x 10^5- 1.7 x 10^7 SARS-CoV-2 RNA cop./ml). Test results ranged from 300 cop./ml, the detection limit for this method, to 1 x 10^8 cop./ml, which is the upper limit of the assay.

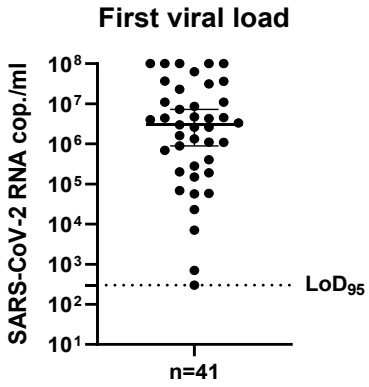


Figure 8 SARS-CoV-2 concentration in the first respiratory specimen obtained from patients. Viral load of respiratory samples collected on the day of admission or within 3 days thereafter from 41 patients (n=41), given as copies per milliliter (cop./ml). The dashed line indicates the limit of detection based on laboratory test accuracy. SARS-CoV-2 RNA, severe acute respiratory syndrome corona virus 2 ribonucleic acid; LoD_{95}, limit of detection 95 percent.

In 25 patients, virions were also detected in the serum, with 20 of them exhibiting viral loads above 300 copies/ml (**Fig. 9A**). Additionally, we analyzed the SARS-CoV-2 variant of concern infecting each patient. Since the COVUR study recruited patients from 2020 to 2022, three patients showed infection with the Wuhan-1 wildtype, while 39.0% were infected with the D614G variant, also known as the European wildtype. Subsequent COVID-19 waves spread the Alpha and Delta variants, which infected more than a third (34.1%), and a fifth of our cohort (19.5%), respectively (**Fig. 9B**).

At hospital admission, 42.5% of patients tested positive for SARS-CoV-2 IgG antibodies (**Fig. 9C**), with only 7.5% (n=3) remaining seronegative by the end of the observation period (**Fig. 9D**). One patient was not tested for SARS-CoV-2 IgG antibodies. Notably, as described above, 46.3% of the cohort received convalescent plasma, providing the patients with the aforementioned antibodies.

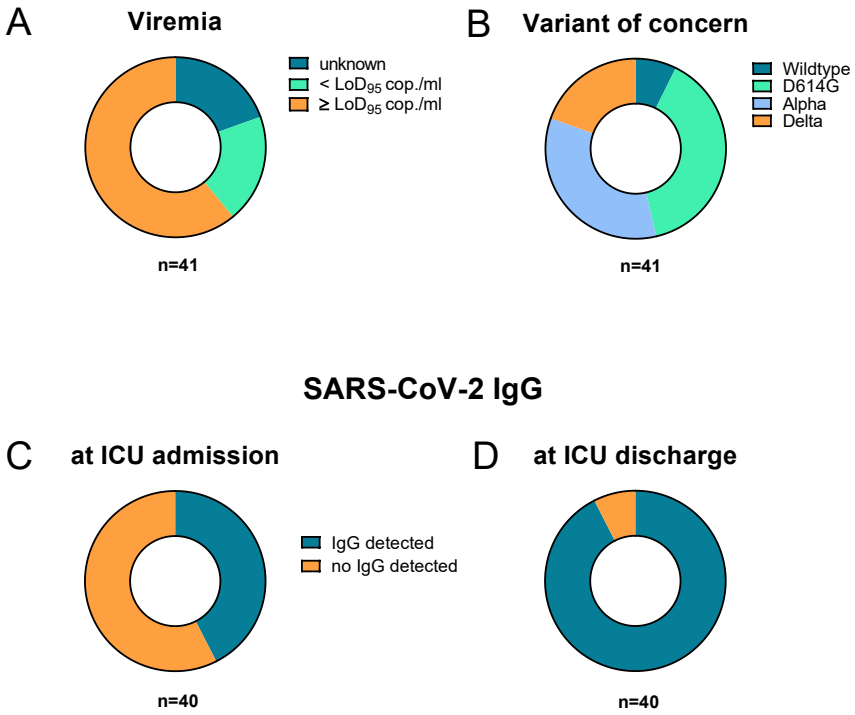


Figure 9 Key characteristics of SARS-CoV-2 infection in the patient cohort. While hospitalized, patients' blood samples were screened for (A) viral load and (B) variant of concern using next generation sequencing. Furthermore, SARS-CoV-2 immunoglobulin G (IgG) levels were monitored at admission (C) and over the course of the disease (D). LoD_{95}, limit of detection 95 percent (300 RNA copies/ml); SARS-CoV-2, severe acute respiratory syndrome corona virus 2; ICU, intensive care unit, reproduced from (Kraft et al. 2026).

5.6. Genome sequencing identifies mutational hotspot in viral polymerase

We used NGS analysis to identify single nucleotide polymorphisms, frameshifts, deletions and other possible genomic alterations by comparing the SARS-CoV-2 genome present at hospital admission to the latest available specimen still harboring viral loads above the laboratory cutoff. In this respect, suitable samples should contain at least 10^4 SARS-CoV-2 RNA copies/ml for proper NGS analysis. We screened for preferably long periods of time in between the specimens, since earlier work from the study group indicated a correlation between the replication period and the occurrence of mutations.

The duration of replication ranged from 6 to 42 days, with a median of 15 days (**Fig. 10A**). Due to the course of disease, most patients showed higher viral loads in the first than in the second sample (**Fig. 10B**). On average, the viral load declined by 1.5 log between compared samples (p<0.0001, Wilcoxon test).

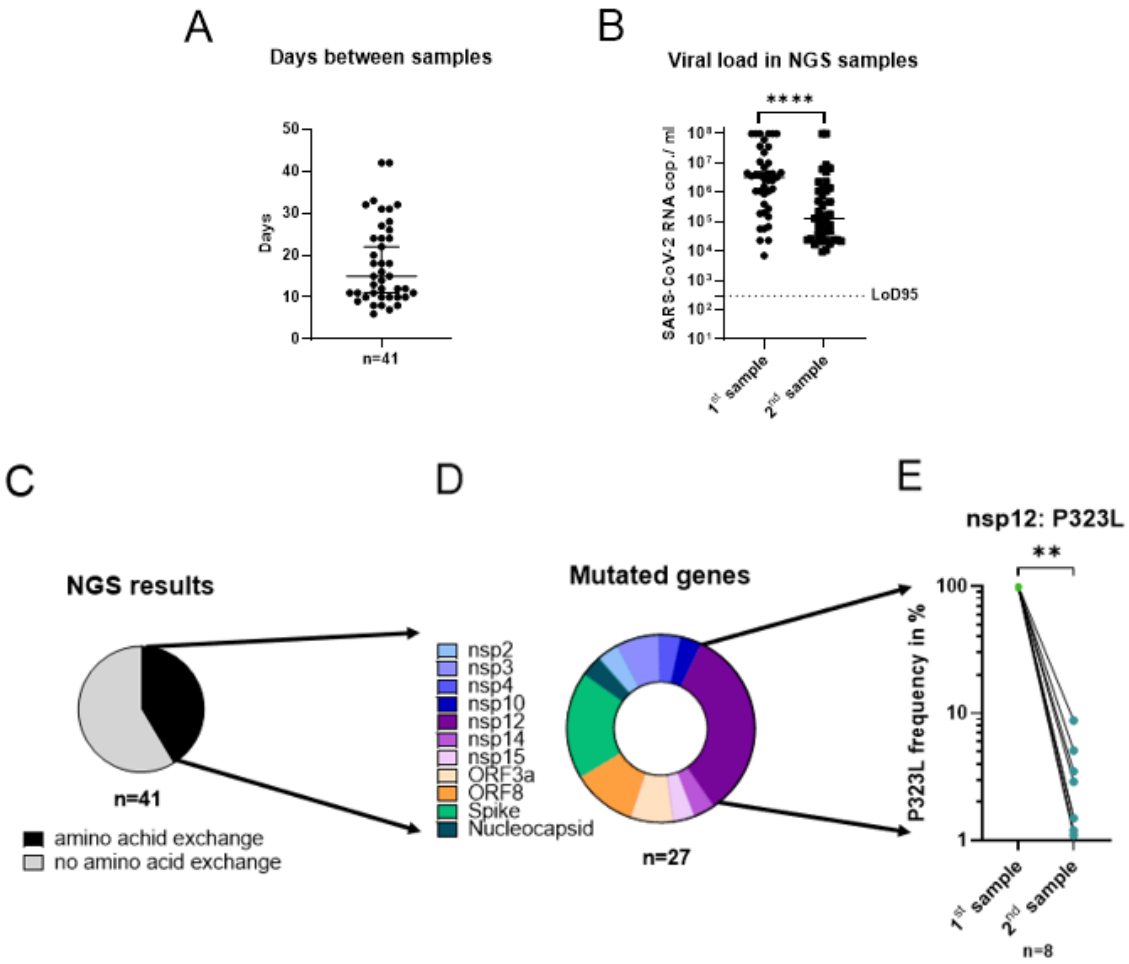


Figure 10 Development of SARS-CoV-2 mutations over time in respiratory samples of hospitalized patients (n=41). (A) Time interval and (B) viral load of the respiratory samples used for next generation sequencing (NGS). Viral loads between the first and second samples were compared using Wilcoxon test. ****p<0.0001. (C-E) Mutational analysis of NGS-derived sequences focusing on the occurrence of mutations (C), the mutated viral gene(s) (D), and the occurrence of the amino acid substitution P323L in non-structural protein 12 (nsp12) (E). The frequency of P323L in the first and second sample was analyzed using Wilcoxon test. *p<0.05, reproduced from (Kraft et al. 2026).

In total we analyzed 87 patient samples, including those from earlier studies performed by Clara Luzia Magnus. The NGS analysis was kindly performed and the results were provided by Dr. Andreas Hiergeist, Institute of Clinical Microbiology and Hygiene, University Hospital Regensburg. Out of 41 analyzed patients, 41% (n=17) showed amino acid exchanges (**Fig. 10C**). Affected RNA segments were the non-structural proteins 2; 3; 4; 10; 12; 14; 15; the open reading frame 3a and 8; and the spike and nucleocapsid protein (**Fig. 10D**). Since eight of the alterations affected the amino acid position 323 of nsp12, we analyzed the frequency with which this single nucleotide polymorphism was detected in the NGS analysis (**Fig. 10E**). In the first samples, the frequency of P323L was near 100% (5x >99%, 2x >98%, 1x >95%), declining to <10% in all follow-up samples over the course of the disease (p=0.0156). The observed percentages, representing proportions of the viral population, can be explained by the presence of viral quasispecies. As the virus is continuously evolving, multiple genetic variants coexist simultaneously. Over time, the variant with the greatest fitness advantage in a given environment tends to outcompete the others. This may generally also account for the disappearance of frameshifts and larger deletions spanning multiple base pairs. This pattern was also observed at other positions. Possible reasons for backmutations, such as various viral fitness advantages, are being discussed further in chapter 6.4.

Table 2 Amino acid exchanges in SARS-CoV-2 genomes identified during the course of COVID-19. The table summarizes the frequency of amino acid substitutions between initial and follow-up samples based on next generation sequencing (NGS) data. Alterations are listed by genomic position and corresponding gene.

Gene	*Amino acid exchange position*	Patient ID	1st NGS sample		2nd NGS sample	
			frequency of mutation	read depth	frequency of mutation	read depth
spike	*T95I*	P35	90.7%	140	7.0%	1384
	G142D	P35	94.7%	403	15.8%	139
	G142D	P38	100%	1387	0.1%	1061
	frameshift: ΔI1183	P9	1.2%	1834	97.2%	5327
	F157S	P12	2.1%	1720	98.6%	2648
Nucleocapsid	Δ46-47	P22	15.2%	1181	6.6%	3150
nsp2	A298T	P29	100%	822	19.0%	662
nsp3	frameshift: ΔE1213	P10	1.4%	1387	100%	515
	L1525F	P17	94.1%	6434	8.5%	543
nsp4	I494V	P38	94.0%	5200	3.1%	2340
nsp10	T4355I	P16	3.3%	3673	98.9%	1066
nsp12	P323L	P19	98.2%	3420	1.5%	3315
	P323L	P22	95.2%	2155	1.1%	1860
	P323L	P26	99.8%	2085	8.8%	2550
	P323L	P27	99.5%	4284	2.9%	1615
	P323L	P33	99.6%	3652	1.2%	2673
	P323L	P34	99.5%	3592	3.5%	1345
	P323L	P36	99.6%	8062	5.1%	651
	P323L	P37	98.3%	1729	1.5%	400
	S4655T	P12	2.2%	1178	99.5%	1609
nsp14	T6303A	P1	0.6%	1165	98.2%	1379
nsp15	S147I	P36	99.8%	8357	2.6%	4374
ORF3a	I20T	P12	3.1%	4324	67.5%	4576
	R68I	P27	98.4%	6789	18.4%	4845
ORF8	Δ100	P17	91.6%	11574	5.1%	1988
	Δ119-120	P36	100%	2894	1.3%	2829
	Δ1526-1537	P17	99.4%	2748	3.1%	1654

Mutations identified in SARS-CoV-2 genome positions are displayed with corresponding sample identifiers. For each genomic position, allele frequencies for mutated sequences, along with read depth values, are shown across all samples. Variant calling was performed using LoFreq with stringent filtering criteria (minimum allele frequency: 1%, minimum read depth: 20×). Functional annotation of identified variants was subsequently conducted using snpEff to determine genomic context and predicted effects on viral proteins. ID, identification number (corresponding to Fig. 6+7)*; NGS*, next generation sequencing; *nsp*, non-structural protein; *ORF*, open reading frame; Δ, deletion at respective amino acid position, reproduced from (Kraft et al. 2026).

We identified 27 amino acid exchanges across 25 different regions in the analyzed genomes. The majority of these amino acid exchanges (21 in total) comprise single nucleotide polymorphisms. We also detected three single base-pair deletions, two of which caused subsequent frameshift mutations, and three deletions spanning multiple amino acids. Overall, *in vivo* evolution shifted viral adaptation more frequently toward wild-type (n=20, 74.1%) than toward mutation (n=7, 25.9%). Considering an NGS error rate of 1%, 11 samples showed no minority variants (frequency >99%

mutation/wildtype at the respective position), representing true reversions. In contrast, 17 samples harbored minority variants (frequency ≤99%) that became dominant in later samples. Thus, both true reversions and outgrowth of minority species occur, with the latter appearing slightly more frequent.

5.7. Epitope mapping reveals varying reasons for amino acid mutations

In our approach to gain insight into the dynamics of antibody and epitope modulation, we further investigated the humoral immune responses to the SARS-CoV-2 spike and nucleocapsid proteins. Overlapping peptides of the Wuhan-1 wildtype genome for these two proteins were immobilized on a chip and incubated with antibodies from patient sera. For this experiment, we selected five patients, who showed genomic alterations in these proteins between the interval samples. We analyzed two samples per patient; one collected before and one after the mutational event.

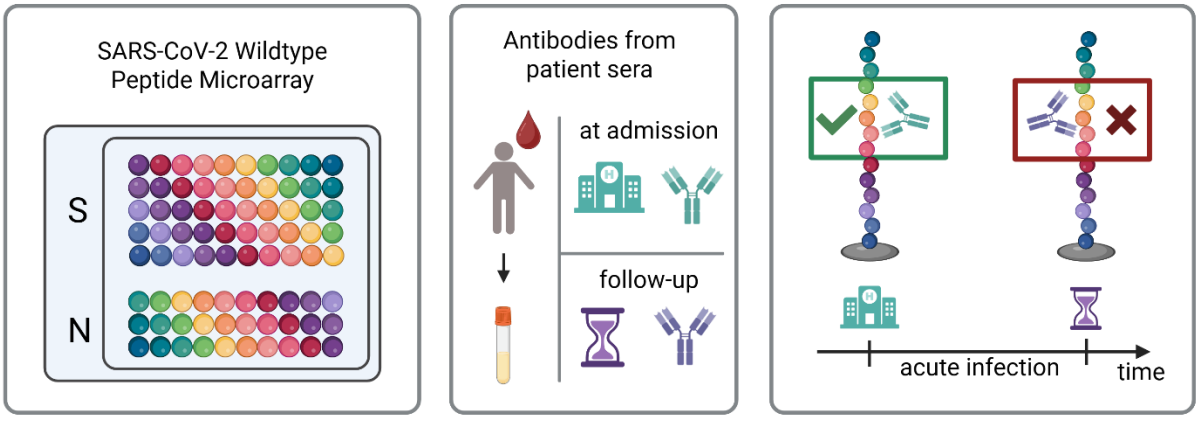


Figure 11 Experimental setup of patient sera antibody reactivity against spike (S) and nucleocapsid (N) epitopes. Schematic overview of the peptide microarray based on the ancestral Wuhan-1 wildtype sequence, consisting of overlapping 15-mer peptides spanning S and N proteins. Serum samples collected at hospital admission and after a median of 15 days (follow-up) were incubated on the array. N, nucleocapsid; SARS-CoV-2, Severe Acute Respiratory Syndrome Coronavirus 2; S, spike.

In all assays, reactivity was assessed exclusively against the Wuhan-1 wild-type sequence printed on the peptide microarray; mutant sequences were not included. Four of the investigated mutational sites (P9 spike fs ΔI1183; P12 spike F157S; P22 nucleocapsid Δ46-47; P35 spike T95I) showed no detectable paratope-epitope interaction in either the first or second sample, suggesting that these epitopes were not immunologically targeted. For one mutational site (spike protein position G142D) two patients exhibited divergent antibody binding patterns. In P35, the epitope remained detectable by immunofluorescence with comparable IgG levels across both time points, including after the patient virus reverted to Wuhan-1 in the follow-up sample. At the same hotspot in P38, the first IgG sample—collected when the patient's virus carried the mutation—showed no binding to the Wuhan-1 wild-type peptide on the array, whereas binding to this wild-type sequence was detected in the second sample. This pattern is compatible with an initial IgG response directed against the mutant epitope that did not cross-react with the Wuhan-1 sequence assayed, followed by antibodies recognizing the wild-type sequence. Possible explanations for the observed antibody binding patterns are discussed in chapter 6.5.

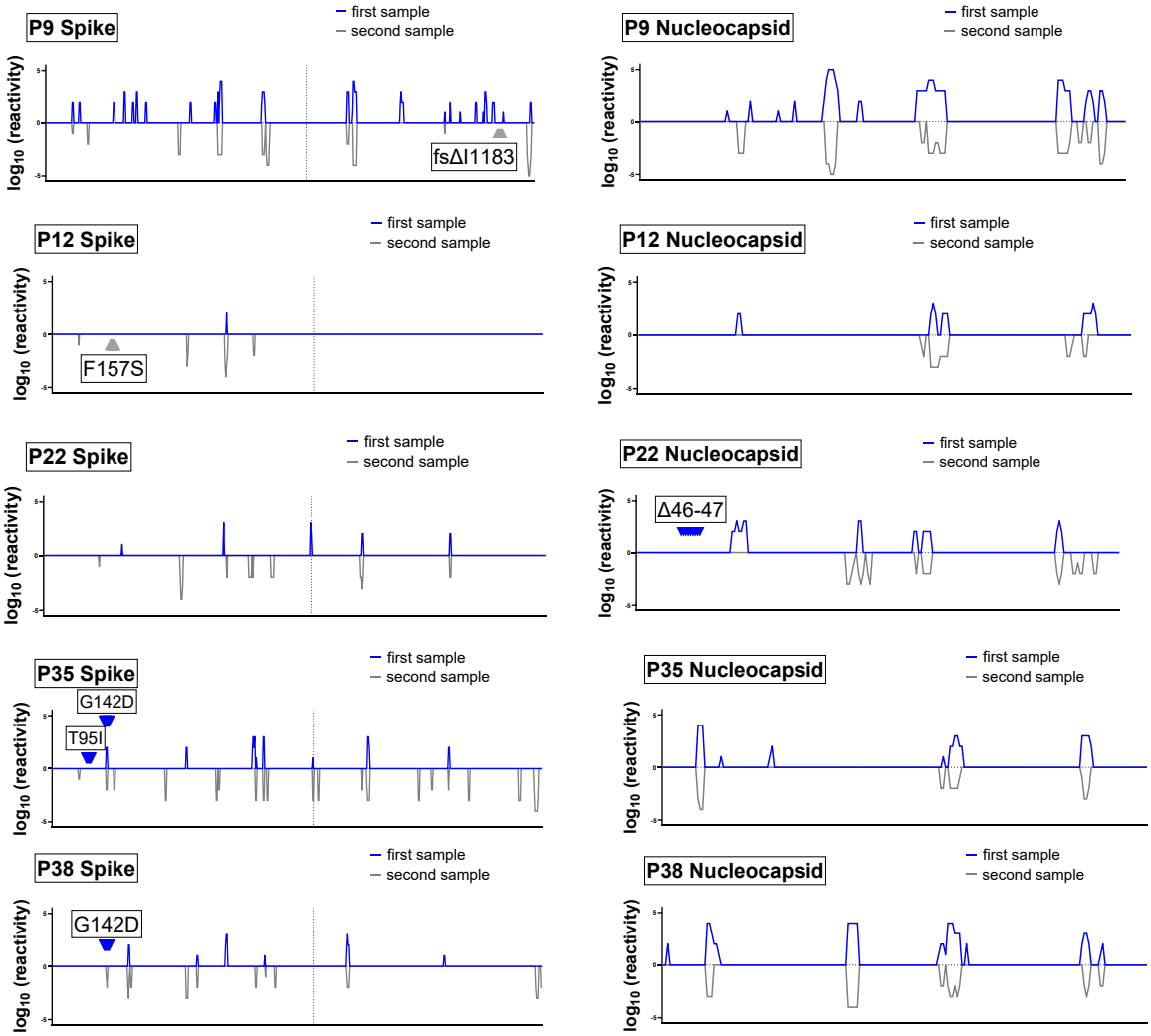


Figure 12 Antibody reactivity of patient sera against SARS-CoV-2 spike (S) and nucleocapsid (N) epitopes. Antibody binding profiles of five individual patients (P) who developed mutations in S or N protein during infection. Reactivity was assessed by immunofluorescence and is presented on a logarithmic scale. Signals above and below baseline represent initial and follow-up samples and are shown in blue and grey, respectively. Arrows indicate mutation sites identified by next generation sequencing, color-coded to match the respective time points. The vertical dashed line denotes the boundary between the S1 and S2 domains of the spike protein. *fs*, frame shift; *Δ*, deletion at the respective amino acid position, adapted from (Kraft et al. 2026).

We compared the number of recognized peptides between the first and second samples and observed an overall increase of antibody activity. In total, 27 additional peptides were identified. However, this difference was not statistically significant (p=0.62), primarily due to one outlier (P9), who showed an opposite trend. Notably, this patient started with the highest number of recognized peptides in the first sample. In the follow-up sample a frameshift mutation emerged at a site within the spike protein that had not been targeted by antibodies in the initial sample. Even after the loss of epitope recognition P9 still exceeded the number of recognized peptides compared to all other patients. It is noteworthy that both P12 and P22 received two doses of convalescent plasma between the first and second sampling time points. The observed discrepancy in epitope recognition may therefore be at least partially attributable to the therapeutic administration of exogenous antibodies.

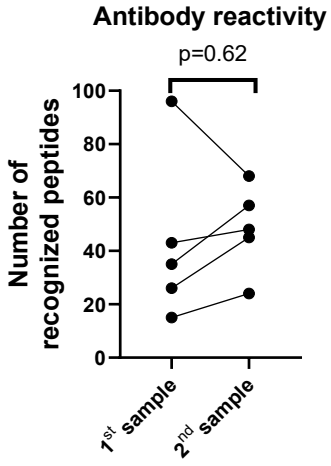


Figure 13 Comparison of the number of recognized peptides among all peptides covering the full-length spike and nucleocapsid protein of SARS-CoV-2 in the first and second patient samples. The number of reactivities against the peptides was extracted from Fig. 9. A total of 27 additional peptides were identified in the second sample compared to the first sample.

5.8. Comparison between patient groups highlights treatment as highly influential on the occurrence of mutations

Figure 14 displays all factors that reached statistically significant p values (<0.05) when comparing patients who developed amino acid exchanges during the course of infection to those whose viral genomes remained unchanged. For detailed odds ratios and p-values, refer to Table 3.

The influence of different therapeutic measures appears to be particularly important. The administration of Remdesivir significantly reduced the occurrence of mutations (Fig 13A). Conversely, the need for ECMO treatment was significantly more frequent in patients who developed amino acid exchanges (Fig 13C). Moreover, the duration of ECMO support was considerably longer in the mutation group compared to those without mutations (Fig 13H). Patients who developed genomic alterations were significantly more likely to require catecholamines at admission (Fig 13B), to experience thrombotic events (Fig 13D) and were significantly younger (Fig 13E), all indicators of severe disease progression. Their viral replication period, defined as time span between analyzed samples, was significantly longer (Fig 13F), likely reflecting the generally extended ICU stay in this group (Fig 13G).

Additionally, the infecting virus variant appeared to influence mutation dynamics: the D614G VOC was significantly less likely to accumulate mutations over the observed timespan, whereas the Delta variant exhibited a significantly higher degree of mutagenicity (Fig 13I).

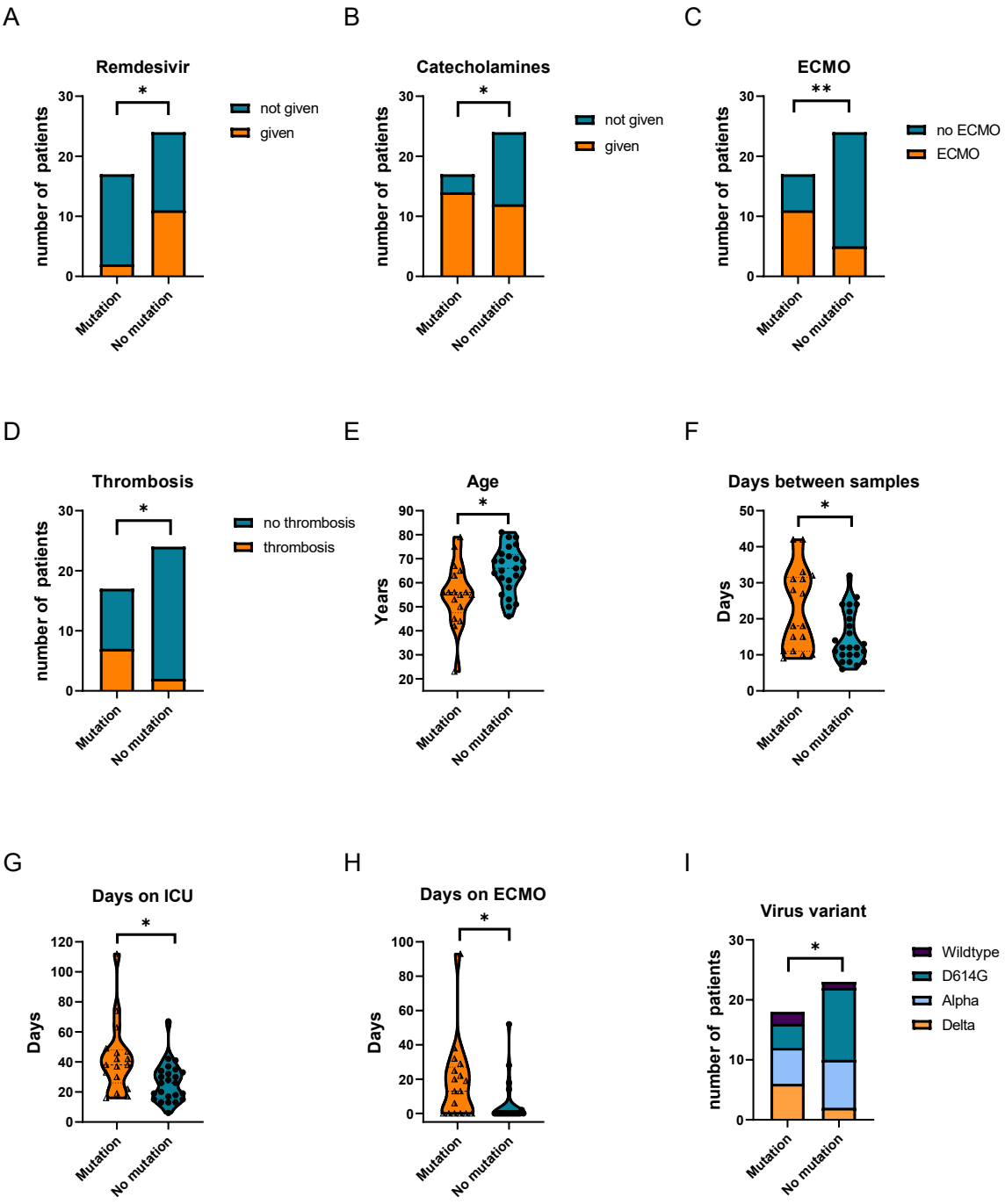


Figure 14 Comparison of patients' samples with and without the development of amino acid exchanges in the SARS-CoV-2 genome during the course of the disease. The samples were compared for (A) the administration of Remdesivir and (B) catecholamines, (C) the use of ECMO, (D) the occurrence of thrombosis, (E) age of patients, (F) interval between samplings, (G) days on ICU, (H) days on ECMO, and (I) virus variant. Only parameters with significant differences were included in the analysis. ECMO, extracorporeal membrane oxygenation; ICU, intensive care unit, reproduced from (Kraft et al. 2026).

5.9. Univariate regression model identifies several significant parameters

Our statistical analysis identified nine parameters that significantly differed between patients who developed genomic alterations and those whose viral genomes remained unchanged: age; time interval between samples used for NGS analysis; virus variant; administration of Remdesivir; need for catecholamine support; length of ICU stay; need for ECMO therapy; ECMO duration; and the occurrence of thrombotic events. These findings suggest that the emergence of mutations is likely driven by a combination of therapeutic interventions (e.g., administration of Remdesivir, catecholamines, and ECMO therapy), severity of disease (as indicated by prolonged ECMO treatment, extended ICU stays, duration of viral replication, and thrombotic complications), and environmental or host-related factors (such as age and the infecting virus variant).

The simultaneous infection with other viral, bacterial or fungal pathogens (parameter: superinfection) further supports the accumulation of parameters indicative of severe disease. Although this factor did not reach statistical significance, it demonstrated a clear trend ($p = 0.081$).

Particular attention should also be given to IgG seropositivity at hospital admission, which exhibited a statistical trend ($p = 0.077$). This parameter is especially noteworthy due to the challenges involved in its interpretation.

Laboratory parameters (D-Dimers, CRP, leucocytes, lymphocytes), despite considerable interindividual variation, showed no statistically significant association with the occurrence of mutational events in our study. The same holds true for the preexisting health conditions we monitored, including organ transplantation, diabetes, hypertension, and COPD.

Table 3 Statistical analyses for collected parameters concerning patient cohort characteristics, medical history, treatment, and outcome. To decipher the factors that correlate significantly with the occurrence of mutational events, both univariate and multivariate regression analysis was performed. The table summarizes the Odds ratios and the p values of the collected parameters for univariate regression.

	Univariate Regression	
Parameter	Odds Ratio (95% CI)	P value
Sex (m/f)	0.492 (0.132-1.837)	0.292
Age (years)	0.918 (0.856-0.984)	0.015
Days between samples used for NGS analysis (days)	1.082 (1.008-1.162)	0.029
Virus variant (Wildtype/ European wildtype/ Alpha/ Delta)	2.295 (1.027-5.132)	0.043
IgG seropositivity at hospital admission (yes/no)	3.265 (0.879-12.128)	0.077
IgG seropositivity in the course of disease (yes/no)	1.524 (0.127-18.324)	0.740
Viral load at ICU admission (RNA copies/ml)	1 (1)	0.108
Viremia (none/<300/>300 RNA copies/ml)	0.697 (0.307-1.581)	0.388
Viremia (none/detectable)	0.338 (0.065-1.754)	0.196
Convalescent plasma therapy (yes/no)	0.462 (0.129-1.657)	0.236
Monoclonal antibody administration (yes/no)	0.667 (0.108-4.134)	0.663
Any immunosuppressive medication (yes/no)	0.650 (0.138-3.068)	0.586
Remdesivir administration (yes/no)	0.158 (0.029-0.845)	0.031
Organ transplantation (yes/no)	1.437 (0.084-24.710)	0.803
Diabetes (yes/no)	0.357 (0.080-1.594)	0.177
Hypertension (yes/no)	0.592 (0.169-2.080)	0.414
COPD (yes/no)	0.0 (0)	0.999
BMI (bodyweight/height in meters^2)	1.009 (0.928-1.097)	0.836
Vaccination (yes/no)	1.437 (0.084-24.710)	0.803
D-Dimers (µg/l)	1.023 (0.958-1.093)	0.502
CRP (mg/l)	1.0 (0.996-1.003)	0.881
Leucocytes (/µl)	1.037 (0.948-1.135)	0.425
Lymphocytes (%)	1.012 (0.909-1.125)	0.832
Lymphocytes (/µl)	1.412 (0.533-3.740)	0.488
Fever (>37.5°C, yes/no)	0.889 (0.256-3.084)	0.853
Catecholamine administration (yes/no)	4.667 (1.061-20.533)	0.042
SOFA Score (0-24 points)	1.148 (0.970-1.357)	0.108
ICU stay (days)	1.062 (1.009-1.118)	0.021
ECMO therapy (yes/no)	6.967 (1.718-28.251)	0.007
ECMO duration (days)	1.058 (1.002-1.116)	0.042
Survival (no/yes)	0.431 (0.108-1.718)	0.233
Prone position (yes/no)	1.833 (0.511-6.571)	0.352
Peripheral thrombotic event and/or pulmonary embolism (yes/no)	4.900 (1.042-23.040)	0.044
Dialysis requirement (yes/no)	0.492 (0.132-1.837)	0.292
Superinfection (yes/no)	4.500 (0.829-24.414)	0.081

BMI, body mass index; CI, confidence interval; COPD, chronic obstructive pulmonary disease; ECMO, extracorporeal membrane oxygenation; f, female; ICU, intensive care unit; IgG, Immunoglobulin G; l, liters; M, male; mg, milligrams; ml, milliliters; NGS, next generation sequencing; RNA, ribonucleic acid; µg, micrograms; SOFA score, sequential organ failure assessment score. Blood type and Rhesus factor were not included in the analysis, because the large number of subgroups precluded a meaningful analysis, adapted from (Kraft et al. 2026).

5.10. Multivariate regression analysis highlights the influence of replication duration and patient age as key factors

To assess the impact of each significant parameter on the dependable variable, the occurrence of mutational events, we performed a multivariate regression analysis using both forward and backward models. Prior to inclusion, all parameters were checked for multicollinearity to ensure independence.

The forward multivariate regression model identified the timespan between analyzed samples, patient age and ECMO therapy as the three most influential factors regarding the occurrence of amino acid exchanges among all variables analyzed. In contrast, the backward model retained the timespan and age, but excluded ECMO therapy, instead including the need for catecholamine administration.

In conclusion, the replication period (p = 0.039-0.042) and patient age (p = 0.016-0.019) emerged as significant factors influencing mutational events during SARS-CoV-2 infection. More precisely, a longer replication interval and younger age were associated with an increased likelihood of amino acid alteration.

Table 4 Multivariate regression analysis. To determine parameters that correlate with mutational events over the course of infection in the patients, forward and backward multivariate regression analysis was used to compare parameters that were statistically significant using univariate regression analysis. The table shows odds ratios and p values for the respective parameters.

	Multivariate Regression (forward)		Multivariate Regression (backward)	
Parameter	*Odds ratio (95% CI)*	*P value*	*Odds ratio (95% CI)*	*P value*
Days between samples used for NGS (days)	1.154 (1.005-1.324)	0.042	1.162 (1.008-1.340)	0.039
Age (years)	0.868 (0.771-0.977)	0.019	0.853 (0.750-0.970)	0.016
ECMO therapy (yes/no)	11.482 (1.702-77.467)	0.012	-	-
Catecholamine administration (yes/no)	-	-	8.214 (0.764-88.327)	0.082

NGS, next generation sequencing; EMCO, extracorporeal membrane oxygenation, adapted from (Kraft et al. 2026).

6. Discussion

6.1. Patient cohort confirms suspected risk factors for severe COVID-19 disease progression

We analyzed a total of 41 patients admitted to the ICU at the University Hospital Regensburg with severe COVID-19 between 2020 and 2022. As Regensburg was designated an ECMO referral center during the SARS-CoV-2 pandemic, it was a center for patients with severe disease progression. While many hospitals discontinued ECMO therapy after 14 days due to little prospect of improvement (Lebreton et al. 2021), Regensburg continued treatment in individual cases for up to 93 days for patients included in our study, if patients were awake, free of neurological deficits, and without severe concomitant organ failure, reflecting the need for prolonged lung recovery in acute respiratory distress syndrome (Wiest et al. 2023). The extended opportunity to observe viral evolution *in vivo* also contributed to improve patient outcomes, particularly for those diagnosed with pulmonary embolism. (Wiest et al. 2024). While a meta-analysis from Germany reported an ECMO-related in-hospital case fatality rate of 65.9% (Friedrichson et al. 2022), our cohort showed a markedly lower mortality rate of 43.8%. Nonetheless, this figure remains considerably above the general infection fatality rate which has been estimated at 0.5-1% (Salzberger et al. 2021). Several factors may account for this discrepancy. Our study was conducted during the early waves of SARS-CoV-2 pandemic, when patients were likely immunologically naïve, having neither vaccine-induced nor infection-acquired immunity. In addition, an increasing number of risk factors has since been identified that appear to predispose individuals to a severe course of the disease.

Compared to the general population in Germany, our cohort showed a disproportionately high percentage of male patients (60.97%). The median age was 61.5 years. These findings are in line with previous studies (Grasselli et al. 2020; Li et al. 2020), which have demonstrated that male sex and advanced age are associated with more severe courses of COVID-19. The median age in our cohort exceeds the German population average of 44.6 years in 2020 (Statistisches Bundesamt 2020, last accessed on January 17th 2026), further supporting age as a risk factor. The median BMI among our patients was 32.6, which corresponds to obesity type II. Notably, the

mean BMI in Germany was 26.0 in 2021 (Statistisches Bundesamt 2021, last accessed on January 17th 2026) showing that our cohort was considerably overweight. In addition, Cai at al. identified not only obesity as an independent risk factor for severe COVID-19, but also a synergistic effect between male sex and obesity. Their findings suggest that obese men are at particularly high risk, even compared to their normal-weight male counterparts (Cai et al. 2020).

6.2. Elevated CRP and D-Dimer levels are prognostic indicators for critical COVID-19

Upon hospital admission, blood samples were obtained from all patients to assess baseline laboratory parameters indicative of disease severity. One key parameter measured was the D-dimer level, a fibrin degradation product that reflects activation of the coagulation cascade. With the exception of two patients, all patients exhibited elevated D-dimer concentrations, consistent with ongoing thrombus formation. The increased occurrence of thromboembolic events during the course of COVID-19 has already been observed by other research groups (Klok et al. 2020). High D-dimer levels have been observed more frequently in non-survivors, suggesting a prognostic value for disease outcome (Tang et al. 2020).

Another parameter indicative of inflammation is CRP, an opsonin produced by the liver in the acute phase of an infection or tissue damage. In our cohort, all patients showed elevated values. In other studies, elevated CRP was associated with more severe COVID-19 courses and may even serve as a predictive marker for clinical deterioration (Tan et al. 2020). In contrast, lymphocyte counts are typically reduced in SARS-CoV-2 infection. The physiological range for lymphocytes lies between 1.18 - 3.74 $x10^3$ cells/µl. In our study, 28 patients showed lymphocytopenia. These findings are consistent with previous reports linking lymphocytopenia to severe outcomes in COVID-19 patients (Guan et al. 2020).

In summary, the combined assessment of these three parameters, D-dimers, CRP and lymphocytes, may serve as an early indicator of the clinical outcome in patients with

SARS-CoV-2 infection. By determining this risk profile at an early stage, the individual therapy could be adapted and thus possibly improve the final outcome.

6.3. IgG positivity at hospitalization detected in the majority of cases

In order to facilitate a comprehensive overview, we plotted the viral loads in respiratory material and serum samples as well as the number of antibodies and the administration of convalescent plasma over time. In most patients, we observed the expected inverse relationship between viral load and antibody concentration, with viral load declining as antibody titers increase (see for example P20). However, this reciprocal pattern is partially constrained by the heterogeneous timing of sample collection. Since sampling was not standardized across patients, temporal resolution of immune and virological dynamics remained suboptimal. Future studies would benefit from predefined, consistent sampling intervals to allow for more accurate monitoring and analysis of infection dynamics.

Another limitation of the study lies in the heterogeneity of different disease stages at the time of hospital admission. Clinical admission is determined by individual factors such as the patient’s subjective symptom perception, comorbidities, and prior medical care. Some patients were transferred from other hospitals after extended pre-treatment, while others experienced rapid disease progression and were admitted to the ICU within hours or days of symptom onset. In particular, the parameters "seropositivity at hospitalization" (which showed a statistical trend, $p=0.077$) and the duration of viral replication (significant with $p=0.029$) are closely linked to this characteristic and must be interpreted in conjunction with it. This variability limits the reliability of our study, but can also be seen as a strength in terms of clinical significance, as it reflects the heterogeneity and unpredictability of real-world patient treatment.

As already mentioned, a special feature of our cohort is the composition of critically ill patients, which is reflected in the high viremia rate observed: while other research groups report viremia in 67% of critically ill patients (Lawrence Panchali et al. 2023),

our cohort showed an even higher proportion at 75%. The cited study also shows a correlation between the disease severity and the level of viremia, suggesting that systemic viral dissemination may serve as a marker for critical illness. While Panchali et al. observed complete clearance of viral RNA from the bloodstream within two weeks in all patients, we detected persistent viremia beyond this time frame in 14 of our patients

In other studies, treatment with convalescent plasma has been associated with clinical benefits such as symptom reduction, improved oxygenation and accelerated clearance of viremia (Duan et al. 2020). In our cohort, 46.3% of patients received at least one dose of convalescent plasma during inpatient treatment. A clear decline in viremia was observed in six of these patients (P10; P11; P12; P13; P21; P22). While the antibody levels increased sharply following plasma administration, a corresponding decrease in respiratory viral load was not observed across all patients in response.

The clinical courses of some patients differed from the overall trends in the cohort, suggesting the presence of patient-specific factors. For example, P1 was the only patient who remained seronegative throughout the entire observation period. This atypical course is even more surprising in view of the fact that, unlike the majority of the cohort (34 patients received immunosuppressive drugs), this patient did not receive any medication that could have impaired antibody production. The patient had no recorded previous illnesses and was admitted in a relatively compensated state with a SOFA score of 1. Nevertheless, he died during the course of the disease. The reasons for this atypical immune response remain speculative. P23 also exhibited only a minimal increase in detectable antibody titers despite receiving three doses of convalescent plasma. This could be explained by the exceptionally high viral load of 1 x 10^8 cop./ml (possibly even higher as this represents the upper limit of detection in our laboratory) that persisted for several days. It is conceivable that the administered antibodies were rapidly sequestered by the large number of circulating virions.

It should be noted that the general therapeutic strategy against SARS-CoV-2 has changed over the course of the study, with increased use of immunosuppressants and antiviral therapy with Remdesivir. Moreover, our results imply that different therapeutic strategies may vary in their effectiveness depending on the viral variant involved. For instance, the administration of dexamethasone appeared to contribute to improved

outcomes among patients infected with the Delta variant (87.5% treated with Dexamethasone, all of which survived). These findings are consistent with the results of the RECOVERY trial, which demonstrated reduced mortality associated with dexamethasone treatment in patients infected with the wild-type, D614G, and Alpha variants (RECOVERY Collaborative Group 2021), as well as with data reported by Afroze et al., who observed particular benefits of dexamethasone therapy in critically ill patients, such as those associated with Delta variant infections (Afroze et al. 2024).

It should also be kept in mind that the different VOCs differ in their mutagenic potential. We observed an amino acid replacement rate of 26.3% (5 out of 19 cases) among the early variants (Wuhan-1 wild type and D614G European wild type), which increased to 42.9% (6 out of 14 cases) for the Alpha variant, and reached 75% (6 out of 8 cases) for the Delta variant. This indicates a progressive increase in mutagenicity among the variants as the pandemic unfolded. Similar findings regarding mutation rates among specific subtypes have been reported in other studies (Ravi et al. 2022; Alam et al. 2022). The mutation dynamics of future SARS-CoV-2 variants therefore remain an important subject for ongoing research.

6.4. Amino acid exchange hotspots detected in spike protein and viral polymerase

To identify gene segments that are subject to viral evolution, two samples per patient were analyzed using whole genome sequencing. Amino acid substitutions were detected in 41% of the patients. The majority of these mutations were located in the spike protein and in non-structural proteins, mainly in nsp12. Notably, nsp12 accounted for 8 out of the 27 mutations observed, highlighting its prominent role and raising the question of why the virus appears to preferentially evolve in this specific region.

In our cohort, the observed mutation in nsp12 is located at amino acid position 323. In the initial sample, all 8 patients carried a Delta variant viral strain with leucine at position 323 in nsp12. In the second sample, however, the same patients exhibited a reversion to proline at this position, thereby aligning once again with the original wildtype sequence. The amino acid substitution at this site of the SARS-CoV-2 genome

was first described in February 2020 and has been associated with an increased accumulation of new mutations (Pachetti et al. 2020). Viruses carrying this substitution appear to be more mutagenic. Experimental studies suggest that this may be linked to conformational changes in the RdRp and the replication complex. Specifically, the presence of leucine at position 323 appears to limit the structural flexibility of the complex, resulting in looser interactions among its components, offering more opportunities for the incorporation of erroneous nucleotides. In addition, replication appears to be faster. Consequently, the P323L mutation is suspected to increase the viral mutation rate through a combination of accelerated replication and decreased fidelity (Alam et al. 2022).

However, this raises the question of why a mutation that appears to be beneficial for the virus, shows a declining trend in our patient cohort. One possible explanation lies in the difference between our patient population and the average public. Kim et. al showed increased transmissibility for viruses with the P323L mutation as well as increased polymerase activity at 33°C compared to 37°C (Kim et al. 2022). A high transmission rate and replication efficiency in the upper respiratory tract – conditions favored by lower temperatures (33°C) – are advantageous for viral spread in the general population. However, in normothermic, ventilated ICU patients, these points become less important, potentially explaining the reduced prevalence in our cohort.

Another advantage conferred by the mutation occurs at the nucleotide level. The P323L substitution results from a cytosine-to-thymidine (C>T) transition, which results in the elimination of a CpG dinucleotide motif (sequence where a cytosine is followed by a guanine). CpG motifs are recognized by toll-like receptors of the innate immune system and can trigger an antiviral immune response (Rahman et al. 2021). By decreasing CpG content, the virus may evade immune detection more effectively, which represents a selective advantage in immunocompetent hosts. However, in our cohort where more than 82% of patients are immunosuppressed, the selective pressure to evade immune recognition via CpG suppression is likely diminished, reducing the relative advantage of this mutation in this specific patient population.

Another argument supporting the occurrence of the reverse mutation is the increased binding affinity of the antiviral agent Remdesivir to the viruses carrying P323L. It binds more strongly to the mutated form of the viral polymerase, potentially enhancing its

inhibitory effect on viral replication (Mohammad et al. 2021). Although no reduced drug sensitivity was observed in a 72-hour experimental setting (Fahnøe et al. 2022), it remains possible that, over prolonged replication periods, viruses lacking the P323L mutation may gain a selective advantage under therapeutic pressure. This hypothesis warrants further investigation in larger patient cohorts. Collectively, these findings suggest that under the specific conditions of critical illness, P323L may confer no selective advantage, resulting in reversion to the ancestral Wuhan-1 wildtype.

Other mutations already described in the literature include T95I; G142D (observed twice) and F157S, all of which are located within the spike protein. All of them decreased in frequency in the follow-up samples. Given the spike protein's critical role in viral entry and its accessibility to the host's immune system, mutations in this area are of particular interest, especially in the context of the production of neutralizing antibodies and vaccines, both of which can be compromised by alterations to the target epitopes. Comprehensive mutational analyses have shown that G142D together with T95I is associated with a high frequency of reverse mutations (Nagaraja et al. 2023), a finding corroborated by our data. The F157S mutation has been identified through bioinformatic modeling as destabilizing, as it appears to reduce the spike protein's affinity for the ACE2 receptor compared to the wild type sequence (Aljindan et al. 2021). These results are consistent with our observation that the F157S mutation was lost in the follow-up sample from the same patient.

In addition, our cohort exhibited 15 mutations not yet described in the current scientific literature (spike: frameshift Δ1526-1537; nucleocapsid: Δ46-47; nsp2 A298T; nsp3 frameshift: ΔE1213, L1525F; mnsp4 I494V; nsp10 T4355I; nsp12 S4655T; nsp14 T6303A; nsp15 S147I; ORF3a I20T, R68I; ORF8: Δ100, Δ119-120, Δ1526-1537). While not yet characterized functionally, several of these mutations have been registered in the GISAID database, which complies SARS-CoV-2 genome sequences submitted from various countries throughout the pandemic. These entries indicate that the mutations have independently occurred across different geographic and temporal contexts, suggesting they are part of the broader mutational landscape of SARS-CoV-2.

Overall, reversions to wild-type (n=20) occurred more frequently than new mutations (n=7). Sixteen samples contained minority variants in the initial sample that later

became dominant, while 11 samples lacked such variants, suggesting true reversions. Thus, both outgrowth of minority species and genuine reversions occur, with the former appearing to be more common.

6.5. Epitope mapping emphasizes individuality of mutations according to course of disease

In order to investigate the impact of the observed mutations on the patients' antibody repertoire and epitope recognition, we performed an epitope mapping experiment. This approach is particularly relevant in the context of potential immune escape variants. Five patients with amino acid substitutions in the spike or nucleocapsid proteins were selected for analysis. Importantly, two patients developed a new mutation between the first and second sample, while the remaining three exhibited a reversion to wild type sequence. To investigate the interaction between patient–derived IgG antibodies and viral epitopes, patient sera were applied to a peptide microarray (CHIP) representing Wuhan-1 wild-type sequences of the SARS-CoV-2 spike and nucleocapsid proteins.

Our studies revealed no altered antibody reactivity toward amino acid substitutions in four patients (P9 spike frameshift ΔI1183; P12 spike F157S; P22 nucleocapsid Δ46-47; P35 spike T95I, G142D). Patient P9 shows high antibody activity in the first measurement. Seven days later, a frameshift mutation at position ΔI1183 of the spike protein was identified. In the second measurement, 17 days after detection of the new frameshift, markedly reduced antibody reactivity was observed. As antibody responses are generally stable, this may indicate selective redistribution to inflamed pulmonary tissue. The frameshift mutation position, represented by the Wuhan-1 wildtype sequence on the CHIP, shows no antibody binding in neither the first nor second sample. Analogous findings were obtained for patient P12, suggesting that the newly acquired F157S mutation in the spike protein likely did not arise as a result of antibody-mediated selection pressure, as the corresponding peptide region was not recognized by patient-derived IgG antibodies – neither before nor after the mutation occurred. Under conditions of immune selection, one would expect antibody binding in the first

sample that is subsequently lost due to an effective escape mutation. However, the experimental setup does not allow for direct assessment of escape efficacy, since the peptide array is based exclusively on the Wuhan-1 wildtype sequence. Patient P22 shows a similar pattern, despite undergoing a reverse mutation. Likewise, patient P35 follows this trend with the T95I mutation, while antibody reactivity at position G142D remained consistent across both time points. In this patient, the previously acquired G142D mutation was lost by the second genome analysis, reverting to wildtype. This most likely reflects the presence of antibodies that recognize an epitope at this site, which is not significantly altered by the glycine-to-aspartic amino acid substitution. Accordingly, the findings argue against successful immune escape mediated by the G142D mutation in the spike protein. A potential explanation for the sustained recognition of both variants is the patient's previous immunization with two doses of the BioNTech vaccine, which primed the patient's immune system to produce antibodies targeting the wildtype virus. These antibodies could either tolerate minor changes within the epitope or bind to adjacent, unaffected regions. In either case, the mutation would not prevent antibody binding.

Interestingly, patient P38 also carries the G142D mutation, but exhibits a different pattern. No antibody reactivity was observed in the first measurement, while a clear response emerged in the second. This suggests a classic case of immune escape: Antibodies present in the patient’s serum during infection with the mutated variant (first sample) did not recognize the corresponding wild-type epitopes. Upon reversion of the mutation (second sample), binding to the wild-type sequence was established. This pattern is consistent with a previously successful immune escape that was subsequently lost. However, it remains unclear why the virus reverted despite the presence of antibodies targeting the wildtype. One possible explanation is that the G142D mutation imposed a functional disadvantage on the virus that outweighed its immune evasion benefit. As already described, a high frequency of reversion mutations at this position has also been reported by other research groups (Nagaraja et al. 2023).

Overall, the CHIP experiment showed that antibody titers rise sharply during and shortly after SARS-CoV-2 infection. In all patients except P9, the later serum sample exhibited broader and stronger antibody reactivity compared to the earlier sample. This suggests either an increased quantity and/or improved affinity maturation of antibodies,

reflecting an intact and functional immune response. These findings are in line with previous studies on the temporal dynamics of antibody development (Zhao et al. 2020; Dittadi et al. 2021). Notably, P12 and P22 received multiple doses of convalescent plasma in between analysis, likely accounting for a proportion of the detected antibodies. In contrast, patient P9 showed a reduced antibody activity in the second measurement, possibly due to redistribution to inflamed pulmonary tissue. Nonetheless, this patient also exhibited new antibody reactivities to peptides that had not been recognized in the first measurement. In summary, the data suggest a progressive refinement and expansion of the antibody response over time.

While antibody responses increased over the course of infection, they appear to have accounted for only a small proportion of the observed amino acid changes. These results indicate that humoral immune pressure was not the dominant force driving intra-host viral evolution in our cohort. It is important to emphasize that our analysis was restricted to linear peptides, which allows assessment only of antibodies recognizing linear epitopes. Consequently, responses targeting conformational or discontinuous epitopes, which may contribute substantially to neutralization, are not captured in this study. Additionally, as our investigation focused primarily on humoral immunity, the potential role of T cell–mediated immune pressure in driving SARS-CoV-2 evolution remains unexplored and warrants further detailed study. Understanding both B cell and T cell contributions will be essential to fully elucidate the mechanisms underlying viral adaptation and immune escape.

6.6. Duration of replication correlates with occurrence of mutation events

After collecting all relevant clinical parameters, we performed a univariate regression analysis to determine the factors that significantly influenced the amino acid substitutions. Variables reaching statistical significance ($p<0.05$) are discussed in detail below. Notably, previously established risk factors for a severe course of the disease, such as gender and obesity, were not significant in our model. While these factors may impact clinical outcomes, they do not appear to influence the occurrence of viral mutations.

One parameter that proved to be significant was treatment with Remdesivir. With a p-value of 0.031, patients who received this medication developed significantly fewer mutations compared to the control group. One possible explanation may lie in the previously described shortening of the recovery period under Remdesivir therapy. A study by Beigel and colleagues (Beigel et al. 2020) reported a difference of 5 days between the treatment and control groups. A slightly smaller difference was also detected in our cohort: the average number of days between the samples used for the NGS was 18.64 days in the control group versus 16.38 days in the patients treated with Remdesivir (n=13). Thus, treatment with Remdesivir reduced the infectious period by nearly two days, thereby limiting the timeframe during which the virus could accumulate mutations via error-prone replication.

The administration of catecholamines at hospitalization also showed a significant association with the occurrence of mutations. This parameter is primarily associated with disease-related circulatory failure and serves as a clinical indicator of disease severity. The development of thrombosis also proved to be statistically significant. Thrombotic events are typically a consequence of intravascular coagulation triggered by the intense inflammatory response frequently observed in critical stages of COVID-19 (Klok et al. 2020; Tang et al. 2020). Ultimately, these factors converge in the equally significant parameter of ECMO therapy, which is employed in cases of severe circulatory failure or insufficient oxygenation of the blood and is itself associated with an increased incidence of thrombotic complications (Lebreton et al. 2021; Campo et al. 2021). This creates a dynamic interplay between circulatory support requirements such as administration of catecholamines, subsequent ECMO treatment—which

increases the risk of thrombosis—and the occurrence of thrombotic events, which impair pulmonary ventilation and place additional stress on the circulatory system, thereby reinforcing the need for ECMO support. Collectively, these parameters may be interpreted under the overarching concept of “disease severity”, which appears to correlate with an elevated likelihood of viral mutations.

The duration of ECMO support and length of ICU stay yielded significant p-values, reflecting the interplay between disease severity, prolonged viral replication, and mutation development. Given the extended disease courses observed in our cohort, patients often required long-term ICU care and, when necessary, ECMO support. A correlation between prolonged replication periods and an increased likelihood of genomic alterations has previously been suggested by our research group (Magnus et al. 2022). Consistently, our current analysis also demonstrates a significant correlation between the length of the sampling interval (which serves as a proxy for extended viral replication) and the increased frequency of amino acid substitutions.

In addition, a significantly higher likelihood of amino acid substitutions was observed in comparatively young patients. The average age in the group developing amino acid exchanges (n=17) was 55.29 years, whereas the median age in the group without mutations (n=24) was 65.42 years. This finding is particularly intriguing given that older age is typically associated with a higher risk of severe disease progression, yet younger patients in our cohort showed an increased probability of mutations. Whether this phenomenon is linked to age-related differences in the immune system remains an open question and warrants further investigation.

In contrast, differences in mutagenicity among the various SARS-CoV-2 VOCs have already been shown in previous studies (Ravi et al. 2022). Our cohort also shows a significant difference in this respect. Later-emerging variants appeared to be more prone to mutations than those closer to the original wild type virus. One possible explanation for this trend is the P323L mutation in the RdRp, which is discussed in more detail in Chapter 6.4. This mutation has been shown to impair the fidelity of the replication process, thereby promoting an increased rate of errors during viral genome replication (Alam et al. 2022).

Following the univariate analysis, we also developed a multivariate regression model to account for potential interdependencies among variables. This approach allows for the identification of parameters that independently contribute to the occurrence of genomic changes. In the forward model, the following variables were conditionally significant for the dependent variable “mutation yes or no”: Days between samples, patient age, and ECMO therapy. In contrast, the backward model identified days between samples, age, and administration of catecholamines at hospital admission as significant predictors. These differences reflect the methodological distinctions between the two approaches, particularly regarding the order in which variables are included in the model. Nevertheless, across both models, all four parameters emerged as significant contributors to the likelihood of mutation occurrence in our cohort.

7. Conclusion

In this study, we investigated the factors that drive and influence the occurrence of amino acid substitutions within the SARS-CoV-2 genome *in vivo*. Our cohort consisted of patients from the ICU of the University Hospital Regensburg and was therefore characterized by a higher disease severity compared to the general population. Key risk factors for a severe course of COVID-19 identified within our cohort included advanced age, male sex, and obesity. The majority of the study group also presented with lymphocytopenia as well as elevated CRP and D-dimer levels upon hospital admission, underscoring the critical nature of their condition. Additionally, the incidence of viremia (75% of the cohort) was markedly above average. In these severe clinical presentations, we observed a reciprocal relationship between viral load and IgG antibody levels, indicating that a representative and functional immune response to SARS-CoV-2 infection did occur in these patients.

Using NGS, we examined the viral genome from two longitudinal samples per patient. Changes in one or more amino acids occurred in 41% of the patients. When comparing the different VOCs, we found an increasing mutation rate from the original wild type to alpha and further to delta. The mutagenic hotspots were primarily located in the spike protein and in nsp12. Particularly notable was the P323L substitution within the viral polymerase (nsp12). In our cohort, eight patients, all infected with the delta variant, exhibited a reverse mutation at this site, reverting from leucine back to the wildtype amino acid, proline.

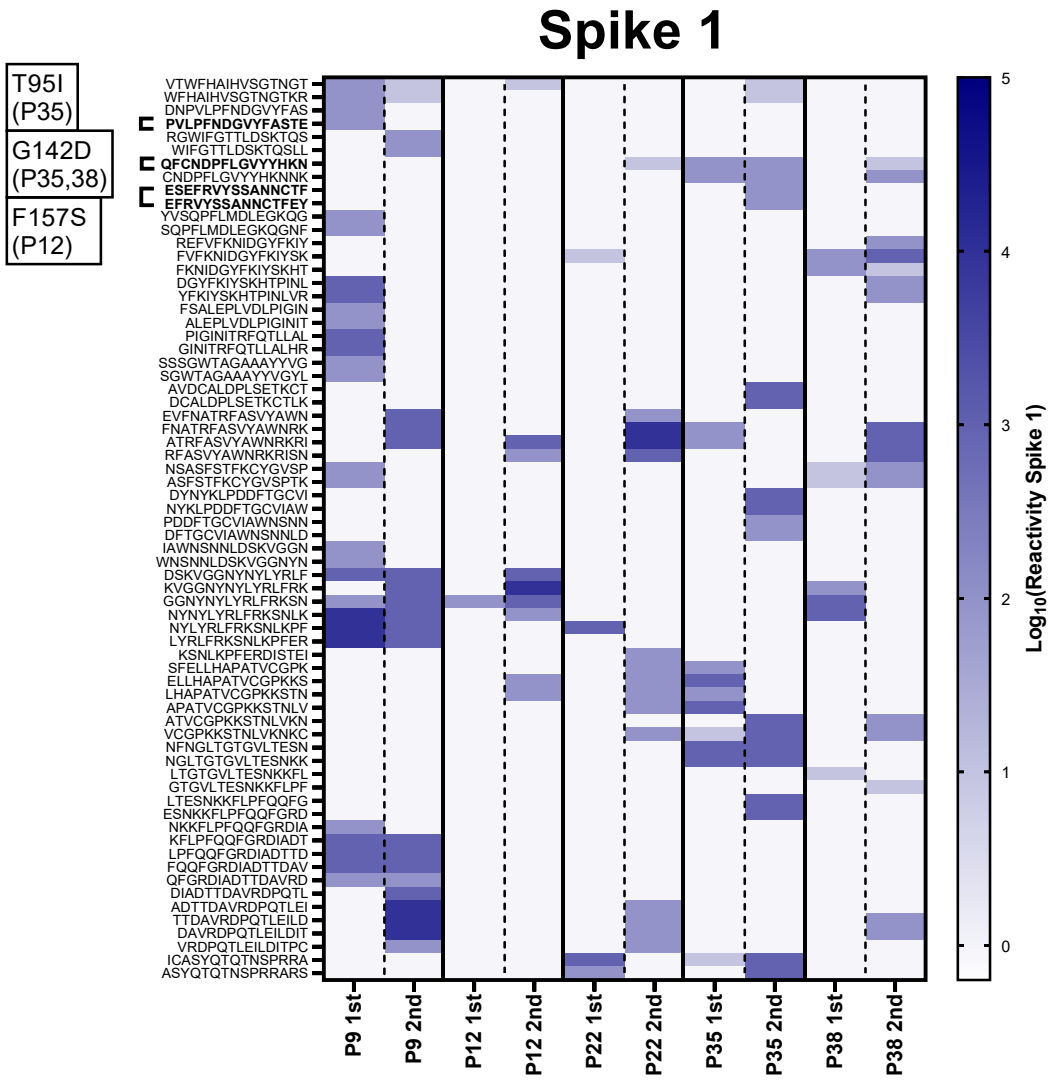
We also analyzed the mutations that occurred in the spike and nucleocapsid proteins for evidence of immune escape driven by antibody-mediated selection pressure. Overall, although antibody responses increased over the course of infection, they appear to have driven only a minority of the observed amino acid changes. These findings suggest that humoral immune pressure was not the primary driver of intra-host viral evolution in most cases. Since this study focused on humoral immunity, the potential contribution of T cell-mediated pressure to SARS-CoV-2 evolution remains to be clarified.

Using statistical regression models, we were able to determine those factors that were significantly associated with amino acid substitutions in the viral genomes. In our analysis, the following parameters were found to be significant: Days between samples (reflecting the viral replication period), length of ICU stay, duration and application of ECMO, younger patient age, virus variant, occurrence of thrombosis, and administration of Remdesivir and catecholamines.

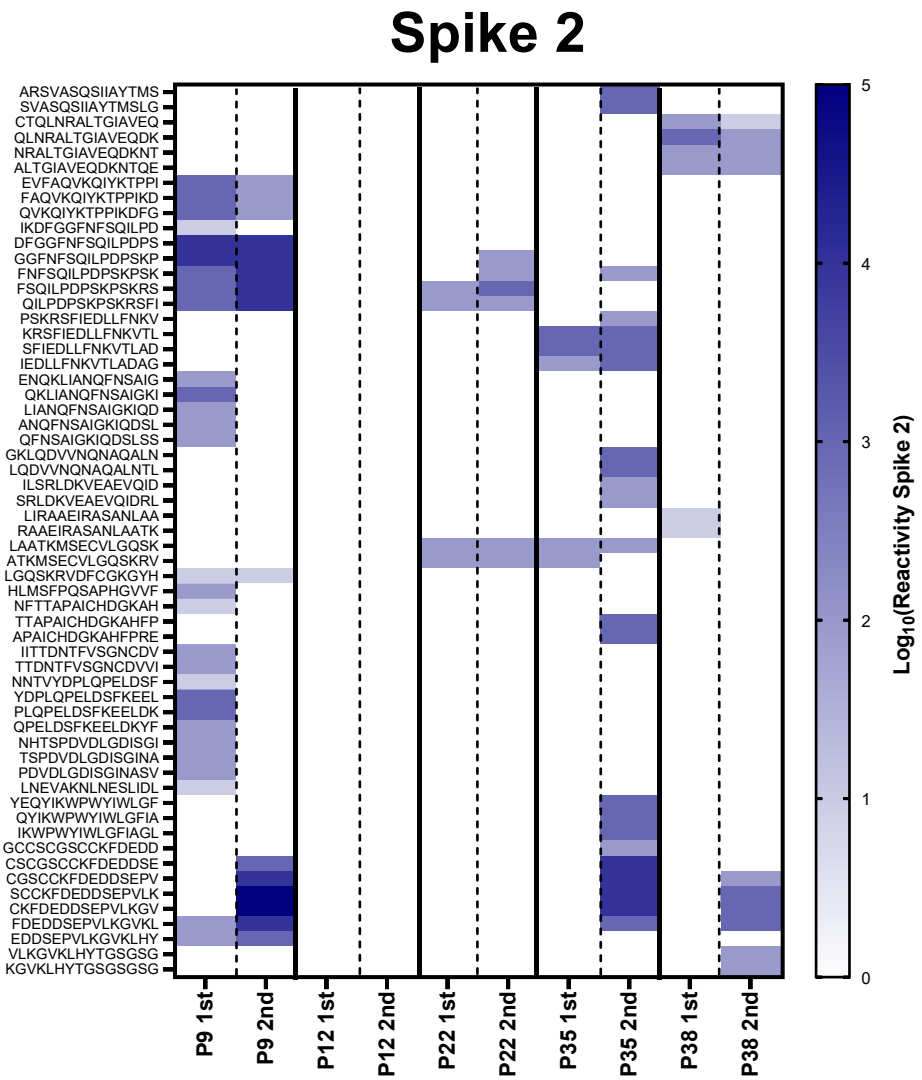
In summary, our study demonstrates that SARS-CoV-2 is capable of adapting to its environment faster than previously assumed, despite its inherent proofreading capabilities. More than one-third of our severely ill patients already exhibited viral genome alterations after an average disease duration of just 15 days. The extent to which these observations can be generalized to the broader development of new SARS-CoV-2 variants, and the role that severe disease progression played in shaping these observations requires further investigation. Nonetheless, our research identified several factors significantly associated with the emergence of genomic mutations.

8. Appendix

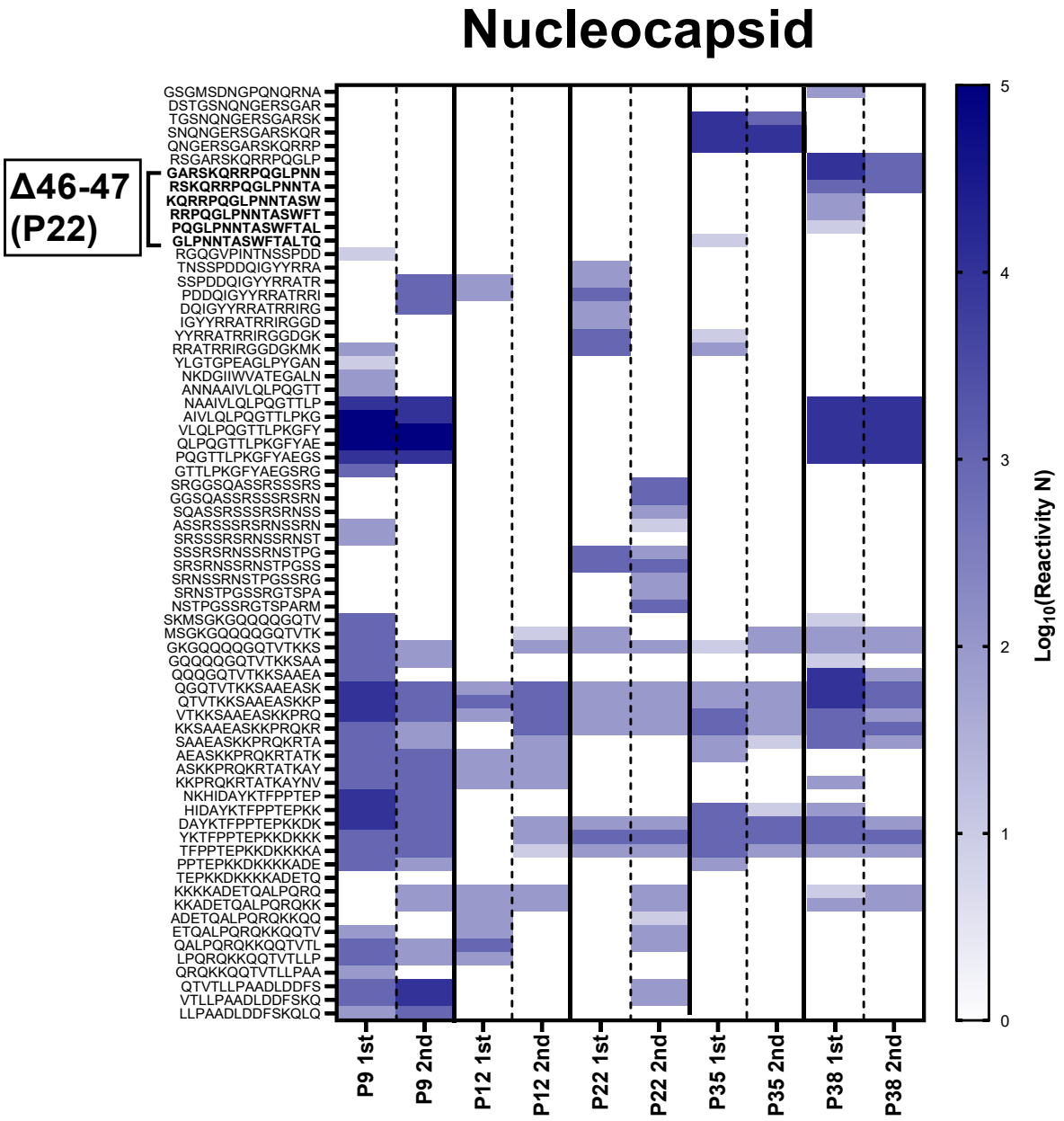
8.1. Supplementary Figures



Supplementary Figure 15 IgG antibody reactivity of patient sera to peptides in the SARS-CoV-2 spike 1 domain. Peptides overlapping the full-length viral genome and immobilized on glass slides were incubated with patients' first and second (follow-up) sera. Binding to the respective peptides was analyzed photometrically, and the reactivity is presented in a color-coded format on a logarithmic scale. The positions of altered amino acids are indicated by black boxes on the left, while the respective peptides are highlighted in bolt font. P, patient; 1st, first; 2nd, second; $\log_{10}$ (decadic logarithm); Δ, deletion at respective amino acid position; fs, frameshift.



Supplementary Figure 16 IgG antibody reactivity of patient sera to peptides in the SARS-CoV-2 spike 2 domain. Peptides overlapping the full-length viral genome and immobilized on glass slides were incubated with patients' first and second (follow-up) sera. Binding to the respective peptides was analyzed photometrically, and the reactivity is presented in a color-coded format on a logarithmic scale. P, patient; 1st, first; 2nd, second; $\log_{10}$ (decadic logarithm).



Supplementary Figure 17 IgG antibody reactivity of patient sera to peptides in the SARS-CoV-2 nucleocapsid protein. Peptides overlapping the full-length viral genome and immobilized on glass slides were incubated with patients' first and second (follow-up) sera. Binding to the respective peptides was analyzed photometrically, and the reactivity is presented in a color-coded format on a logarithmic scale. The positions of altered amino acids are indicated by black boxes on the left, while the respective peptides are highlighted in bolt font. P, patient; 1st, first; 2nd, second; $\log_{10}$ (decadic logarithm); Δ, deletion at respective amino acid position; fs, frameshift.

8.2. List of Figures

Figure 1 Genome organization of SARS-CoV-2

Figure 2 Therapeutic targets and strategies to treat SARS-CoV-2 infection

Figure 3 Clinical characteristics of the patient cohort at admission to the intensive care unit (ICU)

Figure 4 Laboratory parameters at admission of the patient cohort to the intensive care unit (ICU)

Figure 5 Pre-existing conditions, treatments and outcomes of SARS-CoV-2 infection

Figure 6+7 Monitoring of COVID-19 disease progression in hospitalized patients with regard to virological parameters

Figure 8 SARS-CoV-2 concentration in the first respiratory specimen obtained from patients

Figure 9 Key characteristics of SARS-CoV-2 infection in the patient cohort

Figure 10 Development of SARS-CoV-2 mutations over time in respiratory samples of hospitalized patients (n=41)

Figure 11 Experimental setup of patient sera antibody reactivity against spike (S) and nucleocapsid (N) epitopes

Figure 12 Antibody reactivity of patient sera against SARS-CoV-2 spike (S) and nucleocapsid (N) epitopes

Figure 13 Comparison of the number of recognized peptides among all peptides covering the full-length spike and nucleocapsid protein of SARS-CoV-2 in the first and second patient samples

Figure 14 Comparison of patients' samples with and without the development of amino acid exchanges in the SARS-CoV-2 genome during the course of the disease

Supplementary Figure 15 IgG antibody reactivity of patient sera to peptides in the SARS-CoV-2 spike 1 domain

Supplementary Figure 16 IgG antibody reactivity of patient sera to peptides in the SARS-CoV-2 spike 2 domain

Supplementary Figure 17 IgG antibody reactivity of patient sera to peptides in the SARS-CoV-2 nucleocapsid protein

8.3. List of Tables

Table 1 SARS-CoV-2 quantitative RT-qPCR protocol

Table 2 Amino acid exchanges in SARS-CoV-2 genomes identified during the course of COVID-19

Table 3 Statistical analyses for collected parameters concerning patient cohort characteristics, medical history, treatment, and outcome

Table 4 Multivariate regression analysis

8.5. List of abbreviations

ACE2	Angiotensin-converting-enzyme-2
BAL	bronchoalveolar lavage fluid
COPD	chronic obstructive pulmonary disease
CRP	C-reactive protein
COVID-19	Coronavirus Disease 2019
ECMO	extracorporeal membrane oxygenation
ICU	intensive care unit
MERS	Middle East Respiratory Syndrome
NGS	next generation sequencing
Nsp	non-structural protein
ORF	open reading frame
PCR	polymerase chain reaction
Rh	Rhesus factor
RNA	ribonucleic acid
RdRP	RNA-dependent RNA-polymerase
SARS	Severe Acute Respiratory Syndrome
SARS-CoV-2	Severe Acute Respiratory Syndrome Corona Virus 2
SOFA	sequential organ failure assessment
VOC	variants of concern
VOI	variants of interest
VV-ECMO	veno-venous extracorporeal membrane oxygenation
WHO	World Health Organization

Preprint

Kraft T*, Magnus CL*, Hiergeist A, Wenzel JJ, Schuster P, Vogel M, Hanses F, Dienemann T, Schneckenpointner R, Lubnow M, Müller T, Lunz D, Hitzenbichler F, Schmid S, Müller M, Haehnel V, Brosig AM, Offner R, Poeck H, Graf B, Gessner A, Salzberger B, Wiest C, Schmidt B. Back to the wildtype: SARS-CoV-2 evolution in critically ill patients with severe lung failure. Infection. 2025 Oct 8. doi: 10.1007/s15010-025-02650-5. *contributed equally

Literaturverzeichnis

Afroze, Farzana; Begum, Mst Noorjahan; Ahmed, Tahmeed; El Arifeen, Shams; Rahman, Mohammed Ziaur; Rahman, Ahmed Ehsanur et al. (2024): Clinical characterisation, treatment outcomes, and case fatality risk of patients with different SARS-CoV-2 variants in Bangladesh. In: *Journal of global health* 14, S. 5009. DOI: 10.7189/jogh.14.05009.

Alam, A. S. M. Rubayet Ul; Islam, Ovinu Kibria; Hasan, Md Shazid; Islam, Mir Raihanul; Mahmud, Shafi; Al-Emran, Hassan M. et al. (2022): Dominant clade-featured SARS-CoV-2 co-occurring mutations reveal plausible epistasis: An in silico based hypothetical model. In: *Journal of medical virology* 94 (3), S. 1035–1049. DOI: 10.1002/jmv.27416.

Ali, Nurshad (2020): Elevated level of C-reactive protein may be an early marker to predict risk for severity of COVID-19. In: *Journal of medical virology* 92 (11), S. 2409–2411. DOI: 10.1002/jmv.26097.

Aljindan, Reem Y.; Al-Subaie, Abeer M.; Al-Ohali, Ahoud I.; Kumar D, Thirumal; Doss C, George Priya; Kamaraj, Balu (2021): Investigation of nonsynonymous mutations in the spike protein of SARS-CoV-2 and its interaction with the ACE2 receptor by molecular docking and MM/GBSA approach. In: *Computers in Biology and Medicine* 135, S. 104654. DOI: 10.1016/j.compbiomed.2021.104654.

Amicone, Massimo; Borges, Vítor; Alves, Maria João; Isidro, Joana; Zé-Zé, Líbia; Duarte, Sílvia et al. (2022): Mutation rate of SARS-CoV-2 and emergence of mutators during experimental evolution. In: *Evolution, medicine, and public health* 10 (1), S. 142–155. DOI: 10.1093/emph/eoac010.

Beigel, John H.; Tomashek, Kay M.; Dodd, Lori E.; Mehta, Aneesh K.; Zingman, Barry S.; Kalil, Andre C. et al. (2020): Remdesivir for the Treatment of Covid-19 - Final Report. In: *The New England journal of medicine* 383 (19), S. 1813–1826. DOI: 10.1056/NEJMoa2007764.

Biswas, Subrata K.; Mudi, Sonchita R. (2020): Spike protein D614G and RdRp P323L: the SARS-CoV-2 mutations associated with severity of COVID-19. In: *Genomics & informatics* 18 (4), e44. DOI: 10.5808/GI.2020.18.4.e44.

Cai, Qingxian; Chen, Fengjuan; Wang, Tao; Luo, Fang; Liu, Xiaohui; Wu, Qikai et al. (2020): Obesity and COVID-19 Severity in a Designated Hospital in Shenzhen, China. In: *Diabetes Care* 43 (7), S. 1392–1398. DOI: 10.2337/dc20-0576.

Campo, Gianluca; Contoli, Marco; Fogagnolo, Alberto; Vieceli Dalla Sega, Francesco; Zucchetti, Ottavio; Ronzoni, Luca et al. (2021): Over time relationship between platelet reactivity, myocardial injury and mortality in patients with SARS-CoV-2-associated respiratory failure. In: *Platelets* 32 (4), S. 560–567. DOI: 10.1080/09537104.2020.1852543.

Chen, Rita E.; Zhang, Xianwen; Case, James Brett; Winkler, Emma S.; Liu, Yang; VanBlargan, Laura A. et al. (2021): Resistance of SARS-CoV-2 variants to neutralization by monoclonal and serum-derived polyclonal antibodies. In: *Nature medicine* 27 (4), S. 717–726. DOI: 10.1038/s41591-021-01294-w.

Choudhary, Om Prakash; Priyanka; Singh, Indraj; Rodriguez-Morales, Alfonso J. (2021): Second wave of COVID-19 in India: Dissection of the causes and lessons learnt. In: *Travel Medicine and Infectious Disease* 43, S. 102126. DOI: 10.1016/j.tmaid.2021.102126.

Cingolani, Pablo; Platts, Adrian; Le Wang, Lily; Coon, Melissa; Nguyen, Tung; Wang, Luan et al. (2012): A program for annotating and predicting the effects of single nucleotide polymorphisms, SnpEff: SNPs in the genome of Drosophila melanogaster strain w1118; iso-2; iso-3. In: *Fly* 6 (2), S. 80–92. DOI: 10.4161/fly.19695.

Coppo, Anna; Bellani, Giacomo; Winterton, Dario; Di Pierro, Michela; Soria, Alessandro; Faverio, Paola et al. (2020): Feasibility and physiological effects of prone positioning in non-intubated patients with acute respiratory failure due to COVID-19 (PRON-COVID): a prospective cohort study. In: *The Lancet. Respiratory medicine* 8 (8), S. 765–774. DOI: 10.1016/S2213-2600(20)30268-X.

Corman, Victor M.; Landt, Olfert; Kaiser, Marco; Molenkamp, Richard; Meijer, Adam; Chu, Daniel Kw et al. (2020): Detection of 2019 novel coronavirus (2019-nCoV) by real-time RT-PCR. In: *Euro surveillance : bulletin Europeen sur les maladies transmissibles = European communicable disease bulletin* 25 (3). DOI: 10.2807/1560-7917.ES.2020.25.3.2000045.

Davies, Nicholas G.; Abbott, Sam; Barnard, Rosanna C.; Jarvis, Christopher I.; Kucharski, Adam J.; Munday, James D. et al. (2021): Estimated transmissibility and impact of SARS-CoV-2 lineage B.1.1.7 in England. In: *Science (New York, N.Y.)* 372 (6538). DOI: 10.1126/science.abg3055.

Deng, Xianding; Garcia-Knight, Miguel A.; Khalid, Mir M.; Servellita, Venice; Wang, Candace; Morris, Mary Kate et al. (2021): Transmission, infectivity, and neutralization of a spike L452R SARS-CoV-2 variant. In: *Cell* 184 (13), 3426-3437.e8. DOI: 10.1016/j.cell.2021.04.025.

Dittadi, Ruggero; Afshar, Haleh; Carraro, Paolo (2021): Two SARS-CoV-2 IgG immunoassays comparison and time-course profile of antibodies response. In: *Diagnostic Microbiology and Infectious Disease* 99 (4), S. 115297. DOI: 10.1016/j.diagmicrobio.2020.115297.

Drosten, Christian; Günther, Stephan; Preiser, Wolfgang; van der Werf, Sylvie; Brodt, Hans-Reinhard; Becker, Stephan et al. (2003): Identification of a novel coronavirus in patients with severe acute respiratory syndrome. In: *The New England journal of medicine* 348 (20), S. 1967–1976. DOI: 10.1056/NEJMoa030747.

Duan, Kai; Liu, Bende; Li, Cesheng; Zhang, Huajun; Yu, Ting; Qu, Jieming et al. (2020): Effectiveness of convalescent plasma therapy in severe COVID-19 patients. In: *Proceedings of the National Academy of Sciences of the United States of America* 117 (17), S. 9490–9496. DOI: 10.1073/pnas.2004168117.

Essalmani, Rachid; Jain, Jaspreet; Susan-Resiga, Delia; Andréo, Ursula; Evagelidis, Alexandra; Derbali, Rabeb Mouna et al. (2022): Distinctive Roles of Furin and TMPRSS2 in SARS-CoV-2 Infectivity. In: *Journal of virology* 96 (8), e0012822. DOI: 10.1128/jvi.00128-22.

Evolution of SARS-CoV-2 under selection pressure (2021): Evolution of SARS-CoV-2 under selection pressure. Regensburg.

Fahnøe, Ulrik; Pham, Long V.; Fernandez-Antunez, Carlota; Costa, Rui; Rivera-Rangel, Lizandro René; Galli, Andrea et al. (2022): Versatile SARS-CoV-2 Reverse-Genetics Systems for the Study of Antiviral Resistance and Replication. In: *Viruses* 14 (2). DOI: 10.3390/v14020172.

Friedrichson, Benjamin; Kloka, Jan A.; Neef, Vanessa; Mutlak, Haitham; Old, Oliver; Zacharowski, Kai; Piekarski, Florian (2022): Extracorporeal membrane oxygenation in coronavirus disease 2019: A nationwide cohort analysis of 4279 runs from Germany. In: *European journal of anaesthesiology* 39 (5), S. 445–451. DOI: 10.1097/EJA.0000000000001670.

Gallagher, T. M.; Buchmeier, M. J. (2001): Coronavirus spike proteins in viral entry and pathogenesis. In: *Virology* 279 (2), S. 371–374. DOI: 10.1006/viro.2000.0757.

Gorbalenya, Alexander E.; Susan C. Baker; Ralph S. Baric; Raoul J. de Groot; Christian Drosten; Anastasia A. Gulyaeva et al. (2020): The species Severe acute respiratory syndrome-related coronavirus: classifying 2019-nCoV and naming it SARS-CoV-2. In: *Nature microbiology* 5 (4), S. 536–544. DOI: 10.1038/s41564-020-0695-z.

Graham, Mark S.; Sudre, Carole H.; May, Anna; Antonelli, Michela; Murray, Benjamin; Varsavsky, Thomas et al. (2021): Changes in symptomatology, reinfection, and transmissibility associated with the SARS-CoV-2 variant B.1.1.7: an ecological study. In: *The Lancet. Public health* 6 (5), e335-e345. DOI: 10.1016/S2468-2667(21)00055-4.

Grasselli, Giacomo; Zangrillo, Alberto; Zanella, Alberto; Antonelli, Massimo; Cabrini, Luca; Castelli, Antonio et al. (2020): Baseline Characteristics and Outcomes of 1591 Patients Infected With SARS-CoV-2 Admitted to ICUs of the Lombardy Region, Italy. In: *JAMA* 323 (16), S. 1574–1581. DOI: 10.1001/jama.2020.5394.

Gu, Hongjing; Chen, Qi; Yang, Guan; He, Lei; Fan, Hang; Deng, Yong-Qiang et al. (2020): Adaptation of SARS-CoV-2 in BALB/c mice for testing vaccine efficacy. In: *Science (New York, N.Y.)* 369 (6511), S. 1603–1607. DOI: 10.1126/science.abc4730.

Guan, Wei-Jie; Ni, Zheng-Yi; Hu, Yu; Liang, Wen-Hua; Ou, Chun-Quan; He, Jian-Xing et al. (2020): Clinical Characteristics of Coronavirus Disease 2019 in China. In: *The New England journal of medicine* 382 (18), S. 1708–1720. DOI: 10.1056/NEJMoa2002032.

Hähnel, Viola; Peterhoff, David; Bäuerlein, Veronika; Brosig, Andreas-Michael; Pamler, Irene; Johnson, Christian et al. (2020): Manufacturing of convalescent plasma of COVID-19 patients: Aspects of quality. In: *PloS one* 15 (12), e0243967. DOI: 10.1371/journal.pone.0243967.

Hirano, Toshio; Murakami, Masaaki (2020): COVID-19: A New Virus, but a Familiar Receptor and Cytokine Release Syndrome. In: *Immunity* 52 (5), S. 731–733. DOI: 10.1016/j.immuni.2020.04.003.

Hitzenbichler, Florian; Bauernfeind, Stilla; Salzberger, Bernd; Schmidt, Barbara; Wenzel, Jürgen J. (2021): Comparison of Throat Washings, Nasopharyngeal Swabs and Oropharyngeal Swabs for Detection of SARS-CoV-2. In: *Viruses* 13 (4). DOI: 10.3390/v13040653.

Horby, Peter; Lim, Wei Shen; Emberson, Jonathan R.; Mafham, Marion; Bell, Jennifer L.; Linsell, Louise et al. (2021): Dexamethasone in Hospitalized Patients with Covid-19. In: *The New England journal of medicine* 384 (8), S. 693–704. DOI: 10.1056/NEJMoa2021436.

Hu, Ben; Guo, Hua; Zhou, Peng; Shi, Zheng-Li (2021): Characteristics of SARS-CoV-2 and COVID-19. In: *Nature reviews. Microbiology* 19 (3), S. 141–154. DOI: 10.1038/s41579-020-00459-7.

Huang, Chaolin; Wang, Yeming; Li, Xingwang; Ren, Lili; Zhao, Jianping; Hu, Yi et al. (2020): Clinical features of patients infected with 2019 novel coronavirus in Wuhan, China. In: *The Lancet* 395 (10223), S. 497–506. DOI: 10.1016/S0140-6736(20)30183-5.

Iketani, Sho; Liu, Lihong; Guo, Yicheng; Liu, Liyuan; Chan, Jasper F-W; Huang, Yiming et al. (2022): Antibody evasion properties of SARS-CoV-2 Omicron sublineages. In: *Nature* 604 (7906), S. 553–556. DOI: 10.1038/s41586-022-04594-4.

Jo, Dong-Ho; Minn, Dohsik; Lim, Jaegyun; Lee, Ki-Deok; Kang, Yu-Min; Choe, Kang-Won; Kim, Kwang-Nam (2021): Rapidly Declining SARS-CoV-2 Antibody Titers within 4 Months after BNT162b2 Vaccination. In: *Vaccines* 9 (10). DOI: 10.3390/vaccines9101145.

Kemp, Steven A.; Collier, Dami A.; Datir, Rawlings P.; Ferreira, Isabella A. T. M.; Gayed, Salma; Jahun, Aminu et al. (2021): SARS-CoV-2 evolution during treatment of chronic infection. In: *Nature* 592 (7853), S. 277–282. DOI: 10.1038/s41586-021-03291-y.

Khare, Shruti; Gurry, Céline; Freitas, Lucas; Schultz, Mark B.; Bach, Gunter; Diallo, Amadou et al. (2021): GISAID's Role in Pandemic Response. In: *China CDC weekly* 3 (49), S. 1049–1051. DOI: 10.46234/ccdcw2021.255.

Kieninger, Bärbel; Kilger, Magdalena; Foltan, Maik; Gruber, Michael; Lunz, Dirk; Dienemann, Thomas et al. (2023): Prognostic factors for favorable outcomes after veno-venous extracorporeal membrane oxygenation in critical care patients with COVID-19. In: *PloS one* 18 (1), e0280502. DOI: 10.1371/journal.pone.0280502.

Kim, Dongwan; Lee, Joo-Yeon; Yang, Jeong-Sun; Kim, Jun Won; Kim, V. Narry; Chang, Hyeshik (2020): The Architecture of SARS-CoV-2 Transcriptome. In: *Cell* 181 (4), 914-921.e10. DOI: 10.1016/j.cell.2020.04.011.

Kim, Se-Mi; Kim, Eun-Ha; Casel, Mark Anthony B.; Kim, Young-Il; Sun, Rong; Kwack, Mi-Jeong et al. (2022): SARS-CoV-2 variants show temperature-dependent enhanced polymerase activity in the upper respiratory tract and high transmissibility. In: *bioRxiv : the preprint server for biology*. DOI: 10.1101/2022.09.27.509689.

Klok, F. A.; Kruip, M. J. H. A.; van der Meer, N. J. M.; Arbous, M. S.; Gommers, D. A. M. P. J.; Kant, K. M. et al. (2020): Incidence of thrombotic complications in critically ill ICU patients with COVID-19. In: *Thrombosis research* 191, S. 145–147. DOI: 10.1016/j.thromres.2020.04.013.

Korber, Bette; Fischer, Will M.; Gnanakaran, Sandrasegaram; Yoon, Hyejin; Theiler, James; Abfalterer, Werner et al. (2020): Tracking Changes in SARS-CoV-2 Spike: Evidence that D614G Increases Infectivity of the COVID-19 Virus. In: *Cell* 182 (4), 812-827.e19. DOI: 10.1016/j.cell.2020.06.043.

Kraft, Tanja; Magnus, Clara L.; Hiergeist, Andreas; Wenzel, Jürgen J.; Schuster, Philipp; Vogel, Matthias et al. (2026): Back to the wildtype: SARS-CoV-2 evolution in critically ill patients with severe lung failure. In: *Infection* 54 (1), S. 225–242. DOI: 10.1007/s15010-025-02650-5.

Langmead, Ben; Salzberg, Steven L. (2012): Fast gapped-read alignment with Bowtie 2. In: *Nature methods* 9 (4), S. 357–359. DOI: 10.1038/nmeth.1923.

Lauer, Stephen A.; Grantz, Kyra H.; Bi, Qifang; Jones, Forrest K.; Zheng, Qulu; Meredith, Hannah R. et al. (2020): The Incubation Period of Coronavirus Disease 2019

(COVID-19) From Publicly Reported Confirmed Cases: Estimation and Application. In: *Annals of internal medicine* 172 (9), S. 577–582. DOI: 10.7326/M20-0504.

Lawrence Panchali, Merlin Jayalal; Kim, Choon-Mee; Seo, Jun-Won; Kim, Da-Young; Yun, Na-Ra; Kim, Dong-Min (2023): SARS-CoV-2 RNAemia and Disease Severity in COVID-19 Patients. In: *Viruses* 15 (7). DOI: 10.3390/v15071560.

Lebreton, Guillaume; Schmidt, Matthieu; Ponnaiah, Maharajah; Folliguet, Thierry; Para, Marylou; Guihaire, Julien et al. (2021): Extracorporeal membrane oxygenation network organisation and clinical outcomes during the COVID-19 pandemic in Greater Paris, France: a multicentre cohort study. In: *The Lancet. Respiratory medicine* 9 (8), S. 851–862. DOI: 10.1016/S2213-2600(21)00096-5.

Leung, Kathy; Shum, Marcus Hh; Leung, Gabriel M.; Lam, Tommy Ty; Wu, Joseph T. (2021): Early transmissibility assessment of the N501Y mutant strains of SARS-CoV-2 in the United Kingdom, October to November 2020. In: *Euro surveillance : bulletin Europeen sur les maladies transmissibles = European communicable disease bulletin* 26 (1). DOI: 10.2807/1560-7917.ES.2020.26.1.2002106.

Li, Wenhui; Moore, Michael J.; Vasilieva, Natalya; Sui, Jianhua; Wong, Swee Kee; Berne, Michael A. et al. (2003): Angiotensin-converting enzyme 2 is a functional receptor for the SARS coronavirus. In: *Nature* 426 (6965), S. 450–454. DOI: 10.1038/nature02145.

Li, Zhengtu; Yi, Yongxiang; Luo, Xiaomei; Xiong, Nian; Liu, Yang; Li, Shaoqiang et al. (2020): Development and clinical application of a rapid IgM-IgG combined antibody test for SARS-CoV-2 infection diagnosis. In: *Journal of medical virology* 92 (9), S. 1518–1524. DOI: 10.1002/jmv.25727.

Liang, Yanwen; Wang, Mong-Lien; Chien, Chian-Shiu; Yarmishyn, Aliaksandr A.; Yang, Yi-Ping; Lai, Wei-Yi et al. (2020): Highlight of Immune Pathogenic Response and Hematopathologic Effect in SARS-CoV, MERS-CoV, and SARS-Cov-2 Infection. In: *Frontiers in immunology* 11, S. 1022. DOI: 10.3389/fimmu.2020.01022.

Lorenzo-Redondo, Ramon; Nam, Hannah H.; Roberts, Scott C.; Simons, Lacy M.; Jennings, Lawrence J.; Qi, Chao et al. (2020): A clade of SARS-CoV-2 viruses associated with lower viral loads in patient upper airways. In: *eBioMedicine* 62, S. 103112. DOI: 10.1016/j.ebiom.2020.103112.

Magnus, Clara Luzia; Hiergeist, Andreas; Schuster, Philipp; Rohrhofer, Anette; Medenbach, Jan; Gessner, André et al. (2022): Targeted escape of SARS-CoV-2 in vitro from monoclonal antibody S309, the precursor of sotrovimab. In: *Frontiers in immunology* 13, S. 966236. DOI: 10.3389/fimmu.2022.966236.

Minskaia, Ekaterina; Hertzig, Tobias; Gorbalenya, Alexander E.; Campanacci, Valérie; Cambillau, Christian; Canard, Bruno; Ziebuhr, John (2006): Discovery of an RNA virus 3'-5' exoribonuclease that is critically involved in coronavirus RNA synthesis. In: *Proceedings of the National Academy of Sciences of the United States of America* 103 (13), S. 5108–5113. DOI: 10.1073/pnas.0508200103.

Mlcochova, Petra; Kemp, Steven A.; Dhar, Mahesh Shanker; Papa, Guido; Meng, Bo; Ferreira, Isabella A. T. M. et al. (2021): SARS-CoV-2 B.1.617.2 Delta variant replication and immune evasion. In: *Nature* 599 (7883), S. 114–119. DOI: 10.1038/s41586-021-03944-y.

Mohammad, Anwar; Al-Mulla, Fahd; Wei, Dong-Qing; Abubaker, Jehad (2021): Remdesivir MD Simulations Suggest a More Favourable Binding to SARS-CoV-2 RNA Dependent RNA Polymerase Mutant P323L Than Wild-Type. In: *Biomolecules* 11 (7). DOI: 10.3390/biom11070919.

Murphy, Kenneth M.; Weaver, Casey (op. 2017): Jeneway's immunobiology. Unter Mitarbeit von Allan Mowat, Leslie Berg und David Chaplin. 9th ed. New York, London: Garland Science.

Nagaraja, Mudhigeti; Sireesha, Kodavala; Srikar, Anagoni; Sudheer Kumar, Katari; Mohan, Alladi; Vengamma, Bhuma et al. (2023): Mutation Analysis of SARS-CoV-2 Variants Isolated from Symptomatic Cases from Andhra Pradesh, India. In: *Viruses* 15 (8). DOI: 10.3390/v15081656.

Neufeldt, Christopher J.; Joyce, Michael A.; van Buuren, Nicholas; Levin, Aviad; Kirkegaard, Karla; Gale, Michael et al. (2016): The Hepatitis C Virus-Induced Membranous Web and Associated Nuclear Transport Machinery Limit Access of Pattern Recognition Receptors to Viral Replication Sites. In: *PLoS pathogens* 12 (2), e1005428. DOI: 10.1371/journal.ppat.1005428.

Nishiura, Hiroshi; Kobayashi, Tetsuro; Miyama, Takeshi; Suzuki, Ayako; Jung, Sung-Mok; Hayashi, Katsuma et al. (2020): Estimation of the asymptomatic ratio of novel

coronavirus infections (COVID-19). In: *International journal of infectious diseases : IJID : official publication of the International Society for Infectious Diseases* 94, S. 154–155. DOI: 10.1016/j.ijid.2020.03.020.

Ong, Sean Wei Xiang; Chiew, Calvin J.; Ang, Li Wei; Mak, Tze Minn; Cui, Lin; Toh, Matthias Paul H. S. et al. (2022): Clinical and Virological Features of Severe Acute Respiratory Syndrome Coronavirus 2 (SARS-CoV-2) Variants of Concern: A Retrospective Cohort Study Comparing B.1.1.7 (Alpha), B.1.351 (Beta), and B.1.617.2 (Delta). In: *Clinical infectious diseases : an official publication of the Infectious Diseases Society of America* 75 (1), e1128-e1136. DOI: 10.1093/cid/ciab721.

Pachetti, Maria; Marini, Bruna; Benedetti, Francesca; Giudici, Fabiola; Mauro, Elisabetta; Storici, Paola et al. (2020): Emerging SARS-CoV-2 mutation hot spots include a novel RNA-dependent-RNA polymerase variant. In: *Journal of translational medicine* 18 (1), S. 179. DOI: 10.1186/s12967-020-02344-6.

Parkin, Jacqueline; Cohen, Bryony (2001): An overview of the immune system. In: *The Lancet* 357 (9270), S. 1777–1789. DOI: 10.1016/S0140-6736(00)04904-7.

Patone, Martina; Thomas, Karen; Hatch, Rob; Tan, Pui San; Coupland, Carol; Liao, Weiqi et al. (2021): Mortality and critical care unit admission associated with the SARS-CoV-2 lineage B.1.1.7 in England: an observational cohort study. In: *The Lancet. Infectious Diseases* 21 (11), S. 1518–1528. DOI: 10.1016/S1473-3099(21)00318-2.

Perico, Luca; Benigni, Ariela; Casiraghi, Federica; Ng, Lisa F. P.; Renia, Laurent; Remuzzi, Giuseppe (2021): Immunity, endothelial injury and complement-induced coagulopathy in COVID-19. In: *Nature reviews. Nephrology* 17 (1), S. 46–64. DOI: 10.1038/s41581-020-00357-4.

Rahman, Md Marufur; Kader, Shirmin Bintay; Rizvi, S. M. Shahriar (2021): Molecular characterization of SARS-CoV-2 from Bangladesh: implications in genetic diversity, possible origin of the virus, and functional significance of the mutations. In: *Heliyon* 7 (8), e07866. DOI: 10.1016/j.heliyon.2021.e07866.

Ravi, Varsha; Swaminathan, Aparna; Yadav, Sunita; Arya, Hemant; Pandey, Rajesh (2022): SARS-CoV-2 Variants of Concern and Variations within Their Genome Architecture: Does Nucleotide Distribution and Mutation Rate Alter the Functionality and Evolution of the Virus? In: *Viruses* 14 (11). DOI: 10.3390/v14112499.

RECOVERY Collaborative Group (2021): Tocilizumab in patients admitted to hospital with COVID-19 (RECOVERY): a randomised, controlled, open-label, platform trial. In: *Lancet (London, England)* 397 (10285), S. 1637–1645. DOI: 10.1016/S0140-6736(21)00676-0.

Salzberger, Bernd; Buder, Felix; Lampl, Benedikt; Ehrenstein, Boris; Hitzenbichler, Florian; Holzmann, Thomas et al. (2021): Epidemiology of SARS-CoV-2. In: *Infection* 49 (2), S. 233–239. DOI: 10.1007/s15010-020-01531-3.

Snijder, E. J.; Decroly, E.; Ziebuhr, J. (2016): The Nonstructural Proteins Directing Coronavirus RNA Synthesis and Processing. In: *Advances in virus research* 96, S. 59–126. DOI: 10.1016/bs.aivir.2016.08.008.

Snijder, Eric J.; van der Meer, Yvonne; Zevenhoven-Dobbe, Jessika; Onderwater, Jos J. M.; van der Meulen, Jannes; Koerten, Henk K.; Mommaas, A. Mieke (2006): Ultrastructure and Origin of Membrane Vesicles Associated with the Severe Acute Respiratory Syndrome Coronavirus Replication Complex. In: *Journal of virology* 80 (12), S. 5927–5940. DOI: 10.1128/JVI.02501-05.

Statista (2020, last accessed on January 17th 2026): Verteilung der Blutgruppen in Deutschland im Jahr 2020. Online verfügbar unter https://de.statista.com/statistik/daten/studie/251308/umfrage/verteilung-der-blutgruppen-in-deutschland/.

Statistisches Bundesamt, Destatis (2020, last accessed on January 17th 2026): Veränderung des Durchschnittsalters. Online verfügbar unter https://www.giscloud.nrw.de/arcgis/apps/experiencebuilder/experience/?id=5f9809794b46455ca309bd515e8ef184.

Statistisches Bundesamt, Destatis (2021, last accessed on January 17th 2026): Körpermaße der Bevölkerung nach Altersgruppen 2021. Online verfügbar unter https://www.destatis.de/DE/Themen/Gesellschaft-Umwelt/Gesundheit/Gesundheitszustand-Relevantes-Verhalten/Tabellen/koerpermasse-insgesamt.html#fussnote-1-104708.

Stokes, Erin K.; Zambrano, Laura D.; Anderson, Kayla N.; Marder, Ellyn P.; Raz, Kala M.; El Burai Felix, Suad et al. (2020): Coronavirus Disease 2019 Case Surveillance —

United States, January 22–May 30, 2020. In: *Morbidity and Mortality Weekly Report* 69 (24), S. 759–765. DOI: 10.15585/mmwr.mm6924e2.

Tan, Chaochao; Huang, Ying; Shi, Fengxia; Tan, Kui; Ma, Qionghui; Chen, Yong et al. (2020): C-reactive protein correlates with computed tomographic findings and predicts severe COVID-19 early. In: *Journal of medical virology* 92 (7), S. 856–862. DOI: 10.1002/jmv.25871.

Tang, Ning; Li, Dengju; Wang, Xiong; Sun, Ziyong (2020): Abnormal coagulation parameters are associated with poor prognosis in patients with novel coronavirus pneumonia. In: *Journal of thrombosis and haemostasis : JTH* 18 (4), S. 844–847. DOI: 10.1111/jth.14768.

Tzou, Philip L.; Tao, Kaiming; Pond, Sergei L. Kosakovsky; Shafer, Robert W. (2022): Coronavirus Resistance Database (CoV-RDB): SARS-CoV-2 susceptibility to monoclonal antibodies, convalescent plasma, and plasma from vaccinated persons. In: *PloS one* 17 (3), e0261045. DOI: 10.1371/journal.pone.0261045.

Wang, Dawei; Hu, Bo; Hu, Chang; Zhu, Fangfang; Liu, Xing; Zhang, Jing et al. (2020): Clinical Characteristics of 138 Hospitalized Patients With 2019 Novel Coronavirus-Infected Pneumonia in Wuhan, China. In: *JAMA* 323 (11), S. 1061–1069. DOI: 10.1001/jama.2020.1585.

Weinreich, David M.; Sivapalasingam, Sumathi; Norton, Thomas; Ali, Shazia; Gao, Haitao; Bhore, Rafia et al. (2021): REGEN-COV Antibody Combination and Outcomes in Outpatients with Covid-19. In: *The New England journal of medicine* 385 (23), e81. DOI: 10.1056/NEJMoa2108163.

Wiest, Clemens; Philipp, Alois; Foltan, Maik; Geismann, Florian; Schneckenpointer, Roland; Baumgartner, Simon et al. (2024): Refractory circulatory failure in COVID-19 patients treated with veno-arterial ECMO a retrospective single-center experience. In: *PloS one* 19 (4), e0298342. DOI: 10.1371/journal.pone.0298342.

Wiest, Clemens; Philipp, Alois; Lunz, Dirk; Steinmann, Johannes F.; Eissnert, Christoph; Kees, Martin et al. (2023): The Long-Term Support of COVID-19 Patients With Veno-Venous Extracorporeal Membrane Oxygenation. In: *Deutsches Arzteblatt international* 120 (4), S. 56–57. DOI: 10.3238/arztebl.m2022.0354.

Wilm, Andreas; Aw, Pauline Poh Kim; Bertrand, Denis; Yeo, Grace Hui Ting; Ong, Swee Hoe; Wong, Chang Hua et al. (2012): LoFreq: a sequence-quality aware, ultra-sensitive variant caller for uncovering cell-population heterogeneity from high-throughput sequencing datasets. In: *Nucleic acids research* 40 (22), S. 11189–11201. DOI: 10.1093/nar/gks918.

World Health Organization, COVID-19 vaccine tracker (2026, last accessed on January 17th 2026): COVID-19 vaccine tracker and landscape. Online verfügbar unter https://www.who.int/teams/blueprint/covid-19/covid-19-vaccine-tracker-and-landscape.

Wu, Aiping; Peng, Yousong; Huang, Baoying; Ding, Xiao; Wang, Xianyue; Niu, Peihua et al. (2020a): Genome Composition and Divergence of the Novel Coronavirus (2019-nCoV) Originating in China. In: *Cell host & microbe* 27 (3), S. 325–328. DOI: 10.1016/j.chom.2020.02.001.

Wu, Fan; Zhao, Su; Yu, Bin; Chen, Yan-Mei; Wang, Wen; Song, Zhi-Gang et al. (2020b): A new coronavirus associated with human respiratory disease in China. In: *Nature* 579 (7798), S. 265–269. DOI: 10.1038/s41586-020-2008-3.

Xiao, Kangpeng; Zhai, Junqiong; Feng, Yaoyu; Zhou, Niu; Zhang, Xu; Zou, Jie-Jian et al. (2020): Isolation of SARS-CoV-2-related coronavirus from Malayan pangolins. In: *Nature* 583 (7815), S. 286–289. DOI: 10.1038/s41586-020-2313-x.

Xu, Xiaoling; Han, Mingfeng; Li, Tiantian; Sun, Wei; Wang, Dongsheng; Fu, Binqing et al. (2020a): Effective treatment of severe COVID-19 patients with tocilizumab. In: *Proceedings of the National Academy of Sciences of the United States of America* 117 (20), S. 10970–10975. DOI: 10.1073/pnas.2005615117.

Xu, Zhe; Shi, Lei; Wang, Yijin; Zhang, Jiyuan; Huang, Lei; Zhang, Chao et al. (2020b): Pathological findings of COVID-19 associated with acute respiratory distress syndrome. In: *The Lancet. Respiratory medicine* 8 (4), S. 420–422. DOI: 10.1016/S2213-2600(20)30076-X.

Zaki, Ali M.; van Boheemen, Sander; Bestebroer, Theo M.; Osterhaus, Albert D. M. E.; Fouchier, Ron A. M. (2012): Isolation of a novel coronavirus from a man with pneumonia in Saudi Arabia. In: *The New England journal of medicine* 367 (19), S. 1814–1820. DOI: 10.1056/NEJMoa1211721.

Zhao, Juanjuan; Yuan, Quan; Wang, Haiyan; Liu, Wei; Liao, Xuejiao; Su, Yingying et al. (2020): Antibody Responses to SARS-CoV-2 in Patients With Novel Coronavirus Disease 2019. In: *Clinical Infectious Diseases: An Official Publication of the Infectious Diseases Society of America* 71 (16), S. 2027–2034. DOI: 10.1093/cid/ciaa344.

Zhou, Peng; Yang, Xing-Lou; Wang, Xian-Guang; Hu, Ben; Zhang, Lei; Zhang, Wei et al. (2020): Addendum: A pneumonia outbreak associated with a new coronavirus of probable bat origin. In: *Nature* 588 (7836), E6. DOI: 10.1038/s41586-020-2951-z.

Ziegler, Carly G. K.; Allon, Samuel J.; Nyquist, Sarah K.; Mbano, Ian M.; Miao, Vincent N.; Tzouanas, Constantine N. et al. (2020): SARS-CoV-2 Receptor ACE2 Is an Interferon-Stimulated Gene in Human Airway Epithelial Cells and Is Detected in Specific Cell Subsets across Tissues. In: *Cell* 181 (5), 1016-1035.e19. DOI: 10.1016/j.cell.2020.04.035.

Eidesstattliche Erklärung

Ich erkläre hiermit, dass ich die vorliegende Arbeit ohne unzulässige Hilfe Dritter und ohne Benutzung anderer als der angegebenen Hilfsmittel angefertigt habe. Die aus anderen Quellen direkt oder indirekt übernommenen Daten und Konzepte sind unter Angabe der Quelle gekennzeichnet. Insbesondere habe ich nicht die entgeltliche Hilfe von Vermittlungs- bzw. Beratungsdiensten (Promotionsberater oder andere Personen) in Anspruch genommen. Niemand hat von mir unmittelbar oder mittelbar geldwerte Leistungen für Arbeit erhalten, die im Zusammenhang mit dem Inhalt der vorgelegten Dissertation stehen. Die Arbeit wurde bisher weder im In- noch im Ausland in gleicher oder ähnlicher Form einer anderen Prüfungsbehörde vorgelegt.

_____ _____

Ort, Datum Unterschrift